Dimetal Hepta- and Octaalkoxide Anions of Molybdenum and Tungsten, $M_2(OR)_7^-$ and $M_2(OR)_8^{2-}$ (M≡M). Preparation, Structures, Oxidation, and a Study of the Thermal Decomposition of $W_2(OR)_7^-$ to Give $W_2(H)(O)(OR)_6^-$ Where R = ^{t}Bu and ^{i}Pr

T. A. Budzichowski, M. H. Chisholm,* K. Folting, J. C. Huffman, and W. E. Streib

Contribution from the Department of Chemistry and Molecular Structure Center, Indiana University, Bloomington, Indiana 47405

Received December 7, 1994. Revised Manuscript Received April 26, 1995[⊗]

Abstract: The reaction between $M_2(OR)_6$ and KOR in tetrahydrofuran (THF) in the presence of 18-crown-6 leads to the reversible formation of $K(crown)^+M_2(OR)_7^-$ (R = ^{t}Bu, ^{i}Pr) along with $2K^+M_2(OR)_8^{2-}$ for R = $CH_2{}^t$Bu. The anion, $Mo_2(OCH_2{}^t Bu)_7^-$, has one bridging OR ligand whose oxygen atom is distinctly pyramidalized to avoid an unfavorable filled−filled Opπ with M−M π orbital interaction. The Mo−Mo distance, 2.218(1) Å (av), is similar to that in $Mo_2(OCH_2{}^t Bu)_6$ [Chisholm, Cotton Murillo, Reichert *Inorg. Chem.* **1977**, *16*, 1801]. In solution the molecule is fluxional on the NMR time scale even at −78 °C. Other $M_2(OR)_7^-$ anions show similar spectroscopic properties. The dianion is favored for M = W and R = $CH_2{}^t$Bu. The K^+(crown) salts of $M_2(OCH_2{}^t Bu)_8^{2-}$ were structurally characterized (M = Mo and W) and shown to possess a M≡M bonded unit centered with an O_8 "cube". The K^+ ions coordinate four O atoms on opposite faces perpendicular to the M−M vector and are ligated by pyridine when crystals are grown in its presence. The M−M distances 2.33(1) Å (av) (M = W) and 2.256(2) Å (M = Mo) are well within the range seen for $(M{\equiv}M)^{6+}$-containing compounds while the M−O distances are ca. 2.0 Å, notably longer than in $M_2(OR)_6$ compounds, because of (i) their coordination to K^+ and (ii) the increase in coordination number at the metal. Oxidations of the $M_2(OCH_2{}^t Bu)_8^{2-}$ anions with Ph_3PBr_2 cleanly yield $M_2(OCH_2{}^t Bu)_8$ along with KBr and PPh_3. $M_2(OCH_2{}^t Bu)_8$ (M = Mo, W) are essentially insoluble in non-coordinating hydrocarbons but dissolve upon the addition of 1 equiv of pyridine. The $W_2(OR)_7^-$ anions are thermally labile yielding isobutylene (R = ^{t}Bu) or propene (R = ^{i}Pr) and $W_2(\mu\text{-}H)(\mu\text{-}O)(OR)_6^-$. In pyridine-$d_5$ the activation parameters are $\Delta H^\ddagger$ = 23.1(5) kcal/mol and $\Delta S^\ddagger$ = −3.3(5) eu for R = ^{t}Bu and $\Delta H^\ddagger$ = 23.8(8) kcal/mol and $\Delta S^\ddagger$ = −4(2) eu for R = ^{i}Pr. The reactions were first order in $W_2(OR)_7^-$ and independent of added KOR. The kinetic isotope effect k_H/k_D for the protio versus perdeuterio $W_2(O^tBu)_7^-$ complex was 3.5(1) at 23 °C and 3.0(1) at 60.7 °C. From the decomposition of $[W_2(OC(CH_3)(CD_3)_2)_7]^-$ and the ratio of the liberated $CH_2{=}C(CD_3)_2$ to $CD_2{=}C(CH_3)(CD_3)$ the absolute value of k_H/k_D = 3.5(4) at 23 °C. The hydride ligand is chemically inert to olefins and to exchange with the deuterium of ^{t}BuOD. Plausible pathways for the formation of the oxo hydride are discussed and a cyclic transition state akin to a retro-ene reaction is proposed.

Introduction

The $M_2(OR)_6$ (M≡M) compounds are formally coordinatively unsaturated but π-buffered by the presence of the alkoxide ligands.[1] The degree of unsaturation can be tuned by steric factors associated with the R group in such a way as to make a specific $M_2(OR)_6$ compound substrate selective. For example, ethene will react with $W_2(OCH_2{}^t Bu)_6$ but not with $W_2(O^tBu)_6$, and $Mo_2(O^tBu)_6$ does not react with $Ph_2C{=}S$ whereas $Mo_2(OCH_2{}^t Bu)_6$ and $Ph_2C{=}S$ yield $Mo_2(OCH_2{}^t Bu)_6(S)(=CPh_2)$.[2] There are, in fact, numerous such examples but at present little quantitative data are available concerning the details of substrate uptake by $M_2(OR)_6$ complexes. One earlier study provided insight into the reversible binding of CN^- to give $[M_2(OR)_6CN]^-$ compounds.[3] In this paper we study the binding of alkoxide anions to the $M_2(OR)_6$ center. Two new structural types of complexes are reported for d^3−d^3 dimers[4] along with their attendant chemistry. Preliminary communications of some aspects of this work have been published.[5]

Results and Discussion

Syntheses. When **1a**−**f** are mixed with the corresponding KOR in THF or pyridine solution chemically labile equilibria **1** and **2** are rapidly established.

$$\underset{\mathbf{1}}{M_2(OR)_6} + KOR \rightleftharpoons \underset{\mathbf{2}}{K^+[M_2(OR)_7]^-} \quad (1)$$

$$\underset{\mathbf{2}}{K^+[M_2(OR)_7]^-} + KOR \rightleftharpoons \underset{\mathbf{3}}{2K^+[M_2(OR)_8]^{2-}} \quad (2)$$

Compounds **1**, **2**, and **3** are referred to as **a**, **b**, and **c** where M = W and R = ^{t}Bu, ^{i}Pr, and $CH_2{}^t$Bu, respectively, and **d**, **e**, and **f** where M = Mo and R = ^{t}Bu, ^{i}Pr and $CH_2{}^t$Bu, respectively.

[⊗] Abstract published in *Advance ACS Abstracts*, June 15, 1995.

(1) (a) Chisholm, M. H. *Chemtracts: Inorg. Chem.* **1992**, *4*, 273. (b) Caulton, K. G. *New J. Chem.* **1994**, *18*, 25.

(2) (a) Chacon, S. T.; Chisholm, M. H.; Eisenstein, O.; Huffman, J. C. *J. Am. Chem. Soc.* **1992**, *114*, 8497. (b) Budzichowski, T. A.; Chisholm, M. H. Results to be submitted for publication.

(3) Budzichowski, T. A.; Chisholm, M. H. *Polyhedron* **1994**, *13*, 2035.

(4) Chisholm, M. H. *Acc. Chem. Res.* **1990**, *23*, 419.

(5) (a) Budzichowski, T. A.; Chisholm, M. H.; Martin, J. D.; Huffman, J. C.; Moodley, K. G.; Streib, W. E. *Polyhedron* **1993**, *12*, 343. (b) Budzichowski, T. A.; Chisholm, M. H.; Streib, W. E. *J. Am. Chem. Soc.* **1994**, *116*, 389.

0002-7863/95/1517-7428$09.00/0

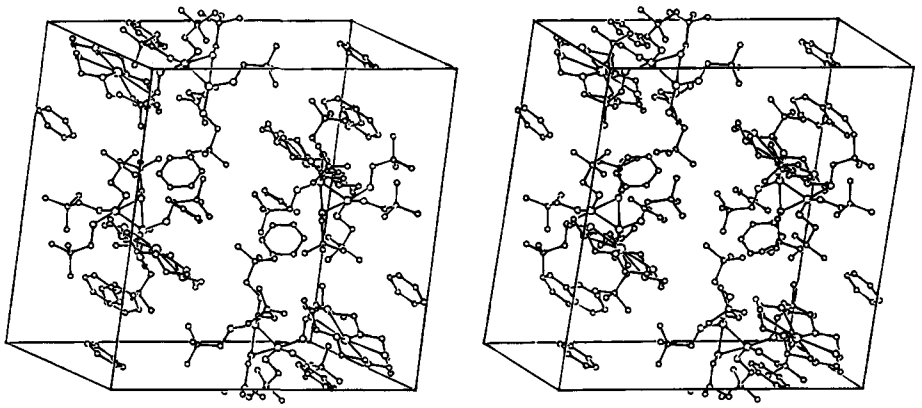

Figure 1. Stereo packing diagram for **2f** showing the disposition of the $[Mo_2(OCH_2{}^tBu)_7]^-$ anions and $[K(18\text{-crown-6})]^+$ cations within the unit cell.

The equilibria are strongly affected by both the nature of the metal and steric considerations. For M = W and R = ^{t}Bu (**1a**) or ^{i}Pr (**1b**) and M = Mo and R = ^{t}Bu (**1d**) or ^{i}Pr (**1e**), the formation of monoanionic "ate" complexes **2a**, **2b**, **2d**, **2e** is strongly favored even in the presence of excess potassium salt. [Thus **3a**, **3b**, **3d**, and **3e** have not been characterized.] In these cases the addition of 18-crown-6 proved especially helpful for preparative scale reactions which proceed cleanly to completion in minutes. One equivalent of this ether is retained during crystallization which is effected by the addition of nonpolar hydrocarbon solvents and/or cooling. The thermal lability of **2a** (described in detail later) necessitated some special precautions. In this case the reaction between 1 equiv of both $W_2(O^tBu)_6$ (**1a**) and KO^tBu is best carried out in THF in the presence of 18-crown-6 at 0 °C. The product may be crystallized by cooling and condensing the solution or it may be isolated simply by evaporating the solvent *in vacuo* (0 °C, 0.01 Torr) and triturating with benzene. The solid material may be stored indefinitely at −34 °C. The $W_2(O^iPr)_7^-$ complex anion was also thermally labile and required similar special precautions for its preparation. In this case $W_2(O^iPr)_6$ had to be prepared fresh at −78 °C and stored cold (<−30 °C) in order to avoid the formation of $W_4(O^iPr)_{12}$ whose equilibrium with $2W_2(O^iPr)_6$ has been previously described.[6] Thus, while the dissociation of $W_4(O^iPr)_{12}$ into $2W_2(O^iPr)_6$ is favored at high temperatures, these conditions prove to be unsuitable for the isolation of $W_2(O^iPr)_7^-$ which thermally decomposes to $[W_2(\mu\text{-H})(\mu\text{-O})(O^iPr)_6]^-$ (*vide infra*).

When M = W and R = $CH_2{}^t$Bu (**1c**), the formation of a dianionic "ate" complex, **3c**, is strongly favored, and the monoanionic derivative **2c** is spectroscopically undetected. One equivalent of $KOCH_2{}^t$Bu and **1c** react in THF to form a 1:1 mixture of **1c**:**3c**, while in pyridine a 1:1 mixture of $W_2(OCH_2{}^t\text{Bu})_6(py)_2$ (**1c**(**py**)$_2$) and **3c** is produced since this solvent reacts with **1c** to form the bis-pyridine adduct. For preparative scale reactions the addition of 18-crown-6 resulted in *lower* crystalline yields and this ether is not retained during crystallization of **3c**. The spectroscopic yield is virtually quantitative (≥95%) so the presence of the crown ether is apparently only detrimental in the sense that it inhibits crystallization of the product.

When M = Mo and R = $CH_2{}^t$Bu (**1f**), the addition of $KOCH_2{}^t$Bu results in the sequential formation of **2f** (1 equiv) and **3f** (≥2 equiv). Thus the formation of a monoanionic "ate" complex is more energetically favorable than a dianionic complex in contrast to what is observed for the analogous tungsten compounds. For preparative scale reactions the addition of 18-crown-6 is helpful during crystallization of **2f** and coordinates the potassium in this derivative (*vide infra*). As was observed for tungsten complex **3c**, the best preparative method for the synthesis of **3f** avoids the introduction of this ether which is not retained during crystallization of the dianionic derivative.

Table 1. Pertinent Bond Distances and Angles for $[K(18\text{-crown-6})]^+[Mo_2(OCH_2{}^tBu)_7]^-$, **2f**

molecule A		molecule B	
	Distance (Å)		
Mo(1)−Mo(2)	2.221(1)	Mo(45)−Mo(46)	2.216(1)
Mo(1)−O(3)	1.951(6)	Mo(45)−O(47)	1.965(6)
Mo(1)−O(9)	1.962(6)	Mo(45)−O(53)	1.921(7)
Mo(1)−O(15)	1.973(6)	Mo(45)−O(59)	1.942(6)
Mo(1)−O(21)	2.155(6)	Mo(45)−O(65)	2.143(6)
Mo(2)−O(21)	2.159(6)	Mo(46)−O(65)	2.144(6)
Mo(2)−O(27)	1.947(6)	Mo(46)−O(71)	1.949(7)
Mo(2)−O(33)	1.931(6)	Mo(46)−O(77)	1.975(6)
Mo(2)−O(39)	1.934(6)	Mo(46)−O(83)	1.968(6)
	Angle (deg)		
O(3)−Mo(1)−O(9)	96.3(3)	O(47)−Mo(45)−O(53)	94.7(3)
O(3)−Mo(1)−O(15)	92.7(3)	O(47)−Mo(45)−O(59)	94.3(3)
O(3)−Mo(1)−O(21)	175.2(3)	O(47)−Mo(45)−O(65)	171.3(3)
O(9)−Mo(1)−O(15	146.9(3)	O(53)−Mo(45)−O(59)	132.6(3)
O(9)−Mo(1)−O(21)	86.9(3)	O(53)−Mo(45)−O(65)	82.4(3)
O(15)−Mo(1)−O(21)	86.5(3)	O(59)−Mo(45)−O(65)	84.7(3)
O(21)−Mo(2)−O(27)	170.1(3)	O(65)−Mo(46)−O(71)	175.8(3)
O(21)−Mo(2)−O(33)	85.5(3)	O(65)−Mo(46)−O(77)	85.6(3)
O(21)−Mo(2)−O(39)	90.9(3)	O(65)−Mo(46)−O(83)	86.6(3)
O(27)−Mo(2)−O(33)	98.9(3)	O(71)−Mo(46)−O(77)	94.5(3)
O(27)−Mo(2)−O(39)	92.6(3)	O(71)−Mo(46)−O(83)	95.5(3)
O(33)−Mo(2)−O(39)	131.5(3)	O(77)−Mo(46)−O(83)	146.5(3)
Mo(1)−O(21)−Mo(2)	62.0(2)	Mo(45)−O(65)−Mo(46)	62.2(2)
ΣX−O(21)−X	318.2(6)	ΣX−O(65)−X	322.2(6)

Solid-State and Molecular Structures. $[K(18\text{-crown-6})]^+[Mo_2(OCH_2{}^tBu)_7]^-$ crystallizes in the space group $P\bar{1}$ in which two complex anions and cations are present in the asymmetric unit along with five molecules of benzene of solvation. A unit cell diagram is given in Figure 1, and this shows the relationship between the cations $[K(18\text{-crown-6})]^+$ and the anions $[Mo_2(OCH_2{}^tBu)_7]^-$ in the solid state. Significantly there is no K^+-to-alkoxide oxygen interaction with the shortest K^+-to-alkoxide O distance being >7.0 Å. The potassium cations are η^6-bound to the crown ether, and a molecule of benzene is found on both sides of this moiety at a distance of ~3.6 Å suggestive of some sort of weak interaction.

Two views of one of the $[Mo_2(OCH_2{}^tBu)_7]^-$ anions are given in Figure 2 along with an atom number scheme that is employed in Table 1 wherein pertinent bond distances and angles are presented. The two anions are very similar as revealed by a careful inspection of the metrical parameters.

(6) (a) Chisholm, M. H.; Clark, D. L.; Folting, K.; Huffman, J. C.; Hampden-Smith, M. J. *J. Am. Chem. Soc.* **1987**, *109*, 7750. (b) Chisholm, M. H.; Clark, D. L.; Hampden-Smith, M. J. *J. Am. Chem. Soc.* **1989**, *111*, 574. (c) Chisholm, M. H.; Clark, D. L.; Folting, K.; Huffman, J. C. *Angew. Chem., Int. Ed. Engl.* **1986**, *25*, 1014.

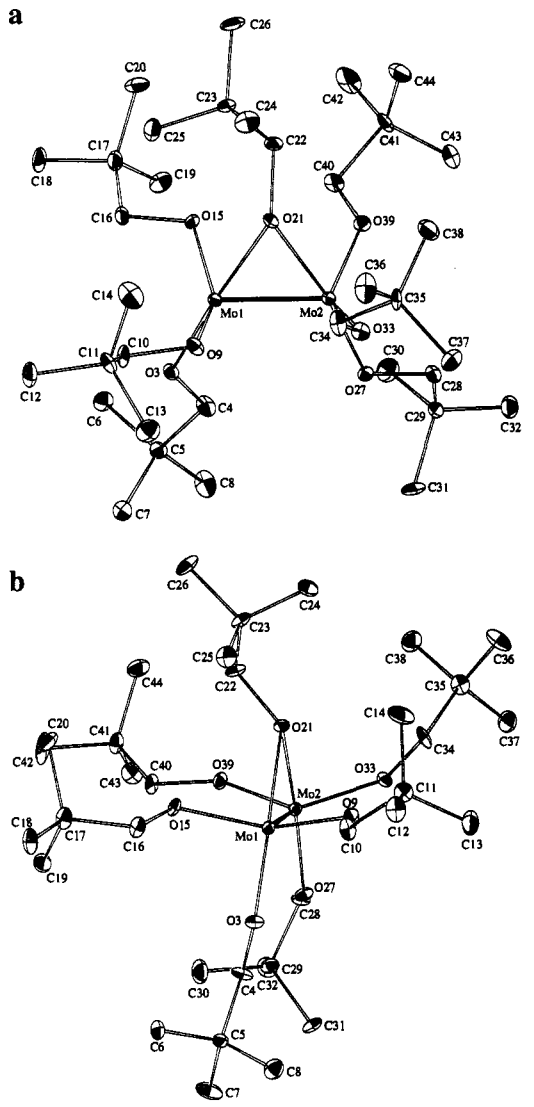

Figure 2. ORTEP drawings for the $[Mo_2(OCH_2{}^tBu)_7]^-$ anion as determined by single-crystal X-ray diffraction. (a) A view perpendicular to the Mo≡Mo bond, and (b) a view along the Mo≡Mo bond. Ellipsoids are shown at the 30% probability level and hydrogen atoms have been omitted for clarity.

The Mo−Mo distance of 2.218(3) Å is comparable to that reported for $Mo_2(OCH_2{}^tBu)_6$, 2.222(2) Å,[7a] indicating that the triple bond remains essentially intact. Each Mo atom is coordinated to four oxygen atoms in a pseudo-trigonal-bipyramidal arrangement wherein one equatorial site is left vacant. The latter site is involved in M−M bonding. Significantly the bridging alkoxide oxygen atom, which occupies an axial position in both trigonal bipyramids, is distinctly pyramidal. The sums of the angles at oxygen, O(3), are 318.6(1)° and 322.2(1)° in the two anions. This is very unusual for bridging alkoxide oxygen atoms that are nearly always planar within ±5°.[8] The Mo−O distances fall into two groups with the longest involving the bridging OR (2.16 Å av). The Mo−O terminal distances span the range 1.92−1.97 Å and are essentially equivalent for the equatorial and axial sites. The Mo−O(3)−Mo angle is rather acute, 62°, as demanded by the short Mo−Mo distance.

$K_2M_2(OCH_2{}^tBu)_8{\cdot}2py$. The molybdenum and tungsten complexes are isomorphous in the space group $P2_1/c$. A single formula unit resides at a general position within the unit cell and there is no crystallographically imposed symmetry.

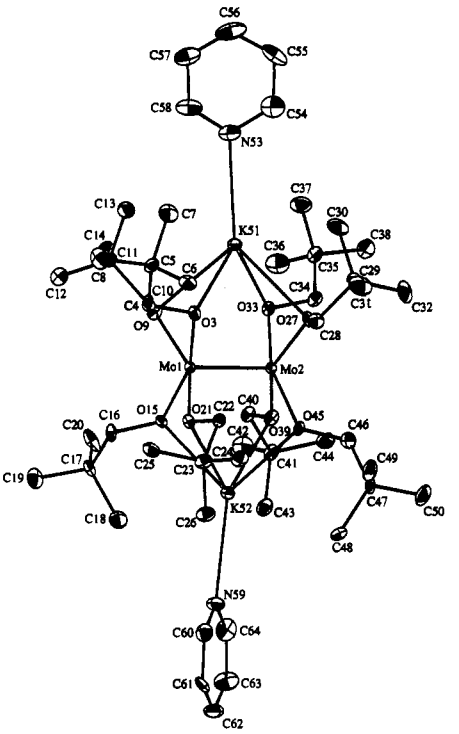

Figure 3. ORTEP drawing of **3f-py$_2$** at the 30% probability level highlighting the coordination geometry of both the Mo and K atoms within the complex. Hydrogen atoms have been omitted for clarity.

A view of the molybdenum complex giving the atom number scheme is shown in Figure 3. The M_2^{6+} unit is encapsulated within a pseudo-O_8 cube and the K^+ ions are each bonded to four O atoms on opposite faces perpendicular to the Mo−Mo vector. In addition, the K^+ ions are ligated to pyridine. It is worth noting that even in the presence of 18-crown-6 the K^+ ions prefer to complex to the $[M_2(OR)_8]^{2-}$ anions and in the absence of pyridine the K^+ positions disorder about opposite faces of the cube.

A view of the complex looking down the W−W axis is given in Figure 4. This shows the eclipsed nature of the two MO_4 units.

Selected bond distances and bond angles are given in Tables 2 and 3, respectively where a comparison is also made between the metrical parameters for the complexes where M = Mo and W.

The M−M distances, 2.26(1) Å (M = Mo) and 2.33(1) Å (M = W), are typical of those associated with $(M{\equiv}M)^{6+}$-containing compounds where the metal ions are ligated to four ligands, e.g. as in $M_2(OR)_6L_2$ complexes.[9] As is typical the W≡W distance is ca. 0.08 Å longer than the Mo≡Mo distance.[10] The M−O distances are 2.00(5) Å (av) and are essentially identical for the two complexes consistent with the fact that the covalent radii of the two elements are virtually identical.[11] The only difference in the distances associated with the central $(M{\equiv}M)^{6+}$ moiety arises from the greater number of core electrons for tungsten.[12] The K-to-O distances span the range 2.63−2.90 Å with no significant difference being observed between the Mo- and W-containing complexes. The M−M−O angles span the range 97−106°.

(7) (a) Chisholm, M. H.; Cotton, F. A.; Murillo, C. A.; Reichert, W. W. *Inorg. Chem.* **1977**, *16*, 1801. (b) Chisholm, M. H.; Folting, K.; Hampden-Smith, M.; Smith, C. A. *Polyhedron* **1987**, *9*, 1747.

(8) Bradley, D. C.; Mehrotra, R. C.; Gaur, D. P. *Metal Alkoxides*; Academic Press: London, 1978.

(9) Akiyama, M.; Chisholm, M. H.; Cotton, F. A.; Extine, M. W.; Haitko, D. A.; Little, D.; Fanwick, P. E. *Inorg. Chem.* **1979**, *18*, 2266.

(10) Chisholm, M. H. *Polyhedron* **1983**, *2*, 681.

(11) Greenwood, N. N.; Earnshaw, A. *Chemistry of the Elements*; Pergamon Press: Oxford, 1989; Chapter 23.

(12) Cotton, F. A.; Walton, R. A. *Multiple Bonds Between Metal Atoms*; Clarendon Press: Oxford, 1993; Chapter 10.

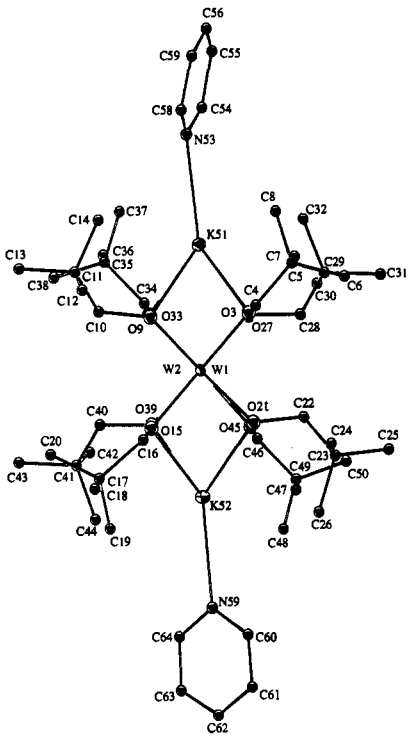

Figure 4. ORTEP drawing of **3c·py₂** at the 30% probability level as viewed directly down the W≡W bond. This view highlights the eclipsed nature of the alkoxide ligands in both **3c·py₂** and **3f·py₂**. Hydrogen atoms have been omitted for clarity.

Table 2. Pertinent Bond Distances (Å) for $K_2M_2(OCH_2{}^tBu)_8{\cdot}py_2$ (M = W, Mo (**3c·py₂**, **3f·py₂**))

$K_2W_2(OCH_2{}^tBu)_8{\cdot}py_2$, **3c·py₂**		$K_2Mo_2(OCH_2{}^tBu)_8{\cdot}py_2$, **3f·py₂**	
W(1)−W(2)	2.335(1)	Mo(1)−Mo(2)	2.257(2)
W(1)−O(3)	2.016(6)	Mo(1)−O(3)	2.003(8)
W(1)−O(9)	1.983(6)	Mo(1)−O(9)	1.987(9)
W(1)−O(15)	2.007(6)	Mo(1)−O(15)	2.004(9)
W(1)−O(21)	1.990(6)	Mo(1)−O(21)	2.010(9)
W(2)−O(27)	1.984(6)	Mo(2)−O(27)	2.000(9)
W(2)−O(33)	2.008(6)	Mo(2)−O(33)	1.992(9)
W(2)−O(39)	1.987(6)	Mo(2)−O(39)	1.988(9)
W(2)−O(45)	2.011(6)	Mo(2)−O(45)	1.995(9)
K−O(av)	2.770(44)	K−O(av)	2.745(33)
K−N(av)	2.886(9)	K−N(av)	2.879(13)

$K_2W_2(OCH_2{}^tBu)_8$. In the absence of pyridine this complex crystallized in the space group $I4_1$. The structure suffers from a compositional disorder wherein the symmetric arrangement of alkoxide ligands supports two different W−W orientations within the O_8 "cube". The essential features of the W_2O_8 unit were as described previously. Similar disorder problems have been observed for related $M_2(OR)_6$ complexes wherein three different metal−metal orientations may be supported within the nondisordered array of alkoxide ligands.[13] [For M^4−M bonded complexes containing an $[M_2X_8]^{n-}$ core there is very commonly a disordering of the M_2 axis within a cube.[14]] Moreover, the metal cations are located above and below the M−M axis as seen in other salts such as $Li_4M_2Me_8$ where M = Mo and W.[14] The metrical parameters for this structural determination differ little from those described above and are given in the supporting information.

(13) (a) Abbott, R. G.; Cotton, F. A.; Falvello, L. R. *Polyhedron* **1990**, *9*, 1821. (b) Chisholm, M. H.; Cook, C. M.; Huffman, J. C.; Streib, W. E. *J. Chem. Soc., Dalton Trans.* **1991**, 929.

(14) (a) Agaskar, P. A.; Cotton, F. A.; Derringer, D. R.; Powell, G. L.; Root, D. R.; Smith, T. J. *Inorg. Chem.* **1985**, *24*, 2786. (b) Cotton, F. A.; Kitagawa, S. *Polyhedron* **1988**, *7*, 463. (c) Cotton, F. A.; Eglin, J. L. *Inorg. Chim. Acta* **1992**, *198–200*, 13 and references therein.

Table 3. Pertinent Bond Angles (deg) for $K_2M_2(OCH_2{}^tBu)_8{\cdot}py_2$ (M = W, Mo (**3c·py₂**, **3f·py₂**))

$K_2W_2(OCH_2{}^tBu)_8{\cdot}py_2$, **3c·py₂**		$K_2Mo_2(OCH_2{}^tBu)_8{\cdot}py_2$, **3f·py₂**	
W(2)−W(1)−O(3)	101.1(2)	Mo(2)−Mo(1)−O(3)	100.5(3)
W(2)−W(1)−O(9)	106.8(2)	Mo(2)−Mo(1)−O(9)	105.8(3)
W(2)−W(1)−O(15)	98.5(2)	Mo(2)−Mo(1)−O(15)	97.5(3)
W(2)−W(1)−O(21)	104.5(2)	Mo(2)−Mo(1)−O(21)	103.9(3)
W(1)−W(2)−O(27)	106.1(2)	Mo(1)−Mo(2)−O(27)	105.3(3)
W(1)−W(2)−O(33)	100.3(2)	Mo(1)−Mo(2)−O(33)	99.3(3)
W(1)−W(2)−O(39)	105.9(2)	Mo(1)−Mo(2)−O(39)	105.2(3)
W(1)−W(2)−O(45)	100.5(2)	Mo(1)−Mo(2)−O(45)	99.6(3)
O(3)−W(1)−O(9)	83.9(3)	O(3)−Mo(1)−O(9)	83.9(4)
O(3)−W(1)−O(15)	160.3(2)	O(3)−Mo(1)−O(15)	162.0(4)
O(3)−W(1)−O(21)	88.4(2)	O(3)−Mo(1)−O(21)	88.5(4)
O(9)−W(1)−O(15)	90.3(2)	O(9)−Mo(1)−O(15)	91.1(4)
O(9)−W(1)−O(21)	148.6(3)	O(9)−Mo(1)−O(21)	150.2(4)
O(15)−W(1)−O(21)	86.8(2)	O(15)−Mo(1)−O(21)	87.3(4)
O(27)−W(2)−O(33)	84.6(2)	O(27)−Mo(2)−O(33)	84.8(4)
O(27)−W(2)−O(39)	148.1(3)	O(27)−Mo(2)−O(39)	149.5(4)
O(27)−W(2)−O(45)	89.9(3)	O(27)−Mo(2)−O(45)	91.0(4)
O(33)−W(2)−O(39)	89.9(2)	O(33)−Mo(2)−O(39)	89.9(4)
O(33)−W(2)−O(45)	159.2(2)	O(33)−Mo(2)−O(45)	161.2(4)
O(39)−W(2)−O(45)	84.2(2)	O(39)−Mo(2)−O(45)	84.4(4)
cis-O−K−O(av)	64.7(27)	*cis*-O−K−O(av)	63.7(20)
trans-O−K−O(av)	98.7(6)	*trans*-O−K−O(av)	96.7(8)
O−K−N(av)	130.5(19)	O−K−N(av)	131.0(23)

Bonding Considerations. The triple bond in $[Mo_2(OR)_8]^{2-}$ anions is readily formulated as $\sigma^2\pi^4$. The eclipsed arrangement of the OR ligands is undoubtedly caused by the binding of the K^+ ions that effectively serve to form bridges. This is in contrast to $M_2(OR)_6L_2$ compounds where L = PMe_3 or pyridine which adopt a staggered geometry in the solid state.[10]

The M−M bonding in the $[M_2(OR)_7]^-$ anions is less intuitively obvious and indeed the $X_3M(\mu\text{-}X)MX_3$ structure with a single bridging group is a new one for d^3−d^3 dimers of molybdenum and tungsten.[4] Nevertheless, the short Mo−Mo distance in $[Mo_2(OCH_2{}^tBu)_7]^-$ is suggestive of the maintenance of a triple bond. One can formulate this from two pseudo-TBP d^3-ML_4 fragments lacking an equatorial site. The frontier orbitals for a TBP ML_4 moiety are known to consist of an **a** and **e** set as shown in **I** below. When the two d^3-ML_4 fragments are brought together to share a common axial bridging site all three orbitals are used to form M−M bonding MOs as depicted in **II** below.

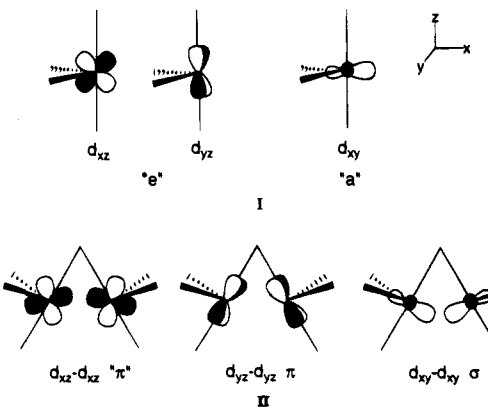

Suffice it to state that six electrons can readily be accommodated in three M−M bonding MO's although the clear characterization of each in terms of σ and π symmetry is more ambiguous.

The point of particular interest concerning the μ-OR ligand is the pyramidal nature of the oxygen atom. Normally μ-OR ligands between metal atoms contain trigonal-planar oxygen atoms.[8] This contrasts with what is observed for trialkyloxo-

nium salts which contain pyramidal oxygen.[15] When early transition metal elements are involved the filled Op_π orbital is often used in π bonding to vacant d_π orbitals.[1] In the present instance, however, a trigonal-planar μ-OR group would introduce a p_π orbital that would interact with the metal d_π orbitals that are involved in M−M bonding as shown in **III** below. This

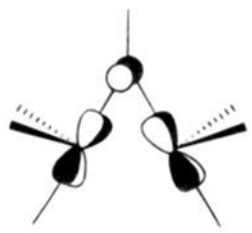

III

would be an unfavorable filled−filled interaction and, to avoid this, the oxygen is rehybridized such that the lone pair is directed away as shown in **IV**. Alternatively one could state that since the μ-OR filled p_π orbital does not find a vacant metal d_π orbital of appropriate symmetry, the μ-OR oxygen atom remains pyramidal.

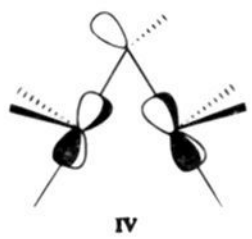

IV

Within the series $M_2(OR)_6$, $[M_2(OR)_7]^-$, and $[M_2(OR)_8]^{2-}$, the terminal M−O distances increase steadily from 1.88 to 1.95 to 2.00 Å consistent with (i) the increase in coordination number at the metal center and (ii) the decrease in Op_π-to-Md_π bonding. The M−M distance is roughly 0.05 Å longer in the dianions $[M_2(OCH_2{}^tBu)_8]^{2-}$ than in the ethane-like $M_2(OR)_6$ compounds[7] but is otherwise comparable to those distances seen in other $M_2(OR)_6L_2$ complexes which have been previously structurally characterized.[10]

Solution-State Properties

NMR Characterization. The K(18-crown-6)$^+[M_2(OR)_7]^-$ complexes are sparingly soluble in aromatic hydrocarbon solvents but extensively soluble in pyridine, tetrahydrofuran (THF), and methylene dichloride. In solution, these complexes show only one type of OR group even at low temperature. It is therefore clear that the monoanions (**2a**−**b**, **2d**−**f**) are fluxional and there must be rapid bridge ⇌ terminal exchange.

For R = ^{t}Bu and M = Mo, the equilibrium between $Mo_2(O^tBu)_6$ and the $[Mo_2(OR)_7]^-$ anion can be observed as a function of temperature in pyridine-d_5. From the values of K_{eq} at various temperatures we determine that $\Delta H° = -23$ kcal/mol and $\Delta S° = -44$ eu for the formation of $[Mo_2(O^tBu)_7]^-$. The equilibrium is chemically rapid but in pyridine-d_5 is slow on the ^{1}H NMR time scale even at 95 °C as evidenced by the lack of line broadening for the signals due to $Mo_2(O^tBu)_6$, $[Mo_2(O^tBu)_7]^-$, and KO^tBu. Although the other monoanions (R ≠ ^{t}Bu) do not appreciably dissociate to give $M_2(OR)_6$ + KOR we can determine that exchange does not occur on the NMR time scale between $M_2(OR)_6$ and $M_2(OR)_7{}^-$ by addition of excess $M_2(OR)_6$.

However, if the solvent is benzene-d_6 or toluene-d_8 then the exchange between $M_2(OR)_6$ and $[Mo_2(OR)_7]^-$ is sufficiently rapid to cause line broadening even at room temperature. This presumably reflects the fact that pyridine is a good donor ligand and that the coordinatively unsaturated $M_2(OR)_6$ compounds actually exist as $M_2(OR)_6(py)_2$ compounds in neat pyridine-d_5.[10] [Several $M_2(OR)_6L_2$ complexes have been structurally characterized.][10] This effectively shuts down the bimolecular exchange of alkoxide ligands between $M_2(OR)_6$ and $[M_2(OR)_7]^-$. Evidence for the bimolecular association of $M_2(OR)_6$ compounds is seen in the reversible coupling of two $W_2(O^iPr)_6$ units to give $W_4(O^iPr)_{12}$ and in the tetranuclear complex $[M_2(O^iPr)_4(\mu\text{-}O^iPr)(\mu\text{-}OMe)]_2$ which contains two localized M−M triple bonds brought together via a pair of μ-O^{i}Pr and μ-OMe ligands.[6,16]

In solution by ^{1}H NMR studies we can see that the $[Mo_2(OR)_7]^-$ anions are favored with respect to disproportionation to give $M_2(OR)_6$ and $[M_2(OR)_8]^{2-}$ with the exception for M = W and R = $CH_2{}^t$Bu. The latter complex is thus unique in the series studied and when R = ^{t}Bu, the $[M_2(OR)_8]^{2-}$ anions are not observed. This finding presumably reflects the steric demands of eight O^{t}Bu ligands at a $(M{\equiv}M)^{6+}$ center.

The $K_2M_2(OR)_8$ complexes show one OR group by ^{1}H NMR spectroscopy as expected based on the solid-state structures described earlier. These compounds are only soluble in donor solvents such as pyridine(-d_5) and THF(-d_8).

UV−Visible Spectra. Whereas the $M_2(OR)_6$ compounds are yellow or orange as a result of the M−M π/δ^* transition tailing into the visible region of the spectrum[17] the $[M_2(OR)_7]^-$ and $[M_2(OR)_8]^{2-}$ anions are blue or purple. The characteristic feature of these complexes is the appearance of an absorption at *ca.* 550 nm with $\epsilon \sim 400$ that is absent in the spectra of the $M_2(OR)_6$ complexes. Details of these and other absorptions are given in the Experimental Section.

The colors of the dianions $[M_2(OR)_8]^{2-}$ are notably less intense than those of the monoanions. For example, for $[W_2(OCH_2{}^tBu)_8]^{2-}$ we observed absorptions at *ca.* 430 ($\epsilon \sim$ 120), 590 ($\epsilon \sim$ 130), and ca. 820 nm ($\epsilon \sim$ 120).

In the case of the $[M_2(OR)_7]^-$ anions that have a bridging OR group, the symmetry of the M_2O_7 core removes the degeneracy of the π_x and π_y orbitals and we may therefore anticipate that a lower energy transition may be seen relative to the ethane-like $M_2(OR)_6$ compounds.

For an isolated $[M_2(OR)_8]^{2-}$ anion in which an $M_2{}^{6+}$ unit is inscribed within a cube of OR^- ligands, the M−M π_x and π_y (and $\pi_x{}^*$ and $\pi_y{}^*$) orbitals will remain degenerate. However, if opposite faces of the cube are capped by K^+ ions this degeneracy will be removed. Moreover, the mixing between π^* and δ^* orbitals that is possible for the ethane-like $M_2(OR)_6$ compounds with D_{3d} symmetry is not possible in the D_{4h}-$[M_2(OR)_8]^{2-}$ systems that have only one M−M δ and δ^* orbital. Thus again we might expect more M−M d based electronic transitions. Certainly, the relatively low molar absorption coefficients seen for the low-energy transitions in the visible and near-IR spectra of $[M_2(OR)_8]^{2-}$ anions are consistent with metal−metal d based electronic transitions but without further careful analysis we cannot offer an assignment. The location of the cations above and below the M−M axis allows the M−M−O angles to be close to 90° as is favored for strong d^n−d^n overlap.

Reactivity

Oxidation. The $K_2M_2(OR)_8$ complexes are cleanly oxidized by Ph_3PBr_2 according to eq 3 in THF. Selection of Ph_3PBr_2 as an oxidant was deemed desirable over Br_2 based on discriminating factors and it was recognized that the PPh_3 byproduct would be innocent.

(15) (a) Lundgren, J. O.; Williams, J. M. *J. Chem. Phys.* **1973**, *58*, 788. (b) Watkins, M. I.; Ip, M. W.; Olah, G. A.; Bau, R. *J. Am. Chem. Soc.* **1982**, *104*, 2365.

(16) Chisholm, M. H.; Hammond, C. E.; Hampden-Smith, M. J.; Huffman, J. C.; Van Der Sluys, W. G. *Angew. Chem., Int. Ed. Engl.* **1987**, *26*, 904.

(17) Chisholm, M. H.; Clark, D. L.; Kober, E. M.; Van Der Sluys, W. G. *Polyhedron* **1987**, *6*, 723.

$$K_2M_2(OR)_8 + Ph_3PBr_2 \xrightarrow[THF]{22\ ^\circ C} M_2(OR)_8 + 2KBr + Ph_3P \quad (3)$$

This provides a new and clean preparation of $Mo_2(OR)_8$ compounds[18] and is also the first preparative route to a $W_2(OR)_8$ compound. It is worth emphasizing that the oxidation reaction, eq 3, does indeed require the presence of the $M_2(OR)_8^{2-}$ dianion if a high yield of $M_2(OR)_8$ is to be formed. Thus, for M = Mo and R = ^{i}Pr, the $[Mo_2(OR)_7]^-$ anion is in equilibrium with $[Mo_2(OR)_8]^{2-}$ and KO^{i}Pr, and the oxidation with Ph_3PBr_2 gives only *ca.* 30% of the known compound $Mo_2(O^iPr)_8$ which is contaminated with a significant amount of $KMo_2(O^iPr)_7Br_2$ (~5%). The latter complex is formed in higher yield when $[Mo_2(O^iPr)_7]^-$ is oxidized by Ph_3PBr_2 in the absence of added KO^{i}Pr. Based on its spectroscopic properties $KMo_2(O^iPr)_7Br_2$ is believed to be related in structure to $Mo_2(OCH_2{}^tBu)_6Br_2(py)$[19] wherein the ligands are arranged in a confacial bioctahedral manner about the Mo centers which are doubly bonded as shown in **V**. In particular the alkoxide ligands for **V** occur in 2:2:1:1:1 ratio based on the C_s symmetry of the

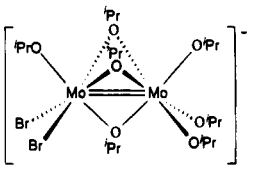

V

molecule with those alkoxides lying off of the mirror plane exhibiting diastereotopic methyl groups (see Experimental Section). For M = W and R = ^{i}Pr, the reaction is similarly complicated. While we observe complete conversion of Ph_3PBr_2 to PPh_3, tractible tungsten-containing species have not yet been isolated or characterized.

In the case of $W_2(OCH_2{}^tBu)_8$, the complex precipitates as a purple solid from THF along with KBr. Addition of 1 equiv of pyridine results in the formation of a toluene-soluble blue-green complex of formula $W_2(OCH_2{}^tBu)_8(py)$ that has been isolated and partially crystallographically characterized. Because the crystals of $W_2(OCH_2{}^tBu)_8(py)$ were extremely thin in one dimension the diffraction data were weak and not of sufficient quantity and quality to allow for a complete refinement. Nevertheless, the essential coordination features of the molecule were revealed: a confacial bioctahedral geometry for the $O_3W(\mu\text{-}O)_3WO_2N$ moiety. This arrangement of ligands is not unprecedented and has been previously observed in a d^2–d^2 dimer of molybdenum, $Mo_2(OCH_2{}^tBu)_6Br_2(py)$, which was prepared by oxidation of $Mo_2(OCH_2{}^tBu)_6$ with $PhCHBr_2$.[19] The coordination of pyridine is readily reversible and the application of a dynamic vacuum to solid samples of $W_2(OCH_2{}^tBu)_8(py)$ results in the reformation of purple insoluble $W_2(OCH_2{}^tBu)_8$.

The $M_2(OCH_2{}^tBu)_8$ complexes where M = Mo and W have essentially identical IR spectra and both are virtually insoluble in non-coordinating solvents. The molybdenum complex is slightly soluble in THF, probably because the molybdenum atoms are less Lewis acidic and can be prepared independently by the alcoholysis of $Mo(NMe_2)_4$.

Our isolation of $W_2(OCH_2{}^tBu)_8(py)$ and the insolubility of $M_2(OCH_2{}^tBu)_8$ complexes lead us to suggest that they are polymeric in the solid state. Indeed one can envisage two plausible and appealing polymeric structures. One involves the formation of singly bridged confacial bioctahedral W_2O_9 units as shown in **VI** and the other involves edge-shared bioctahedra

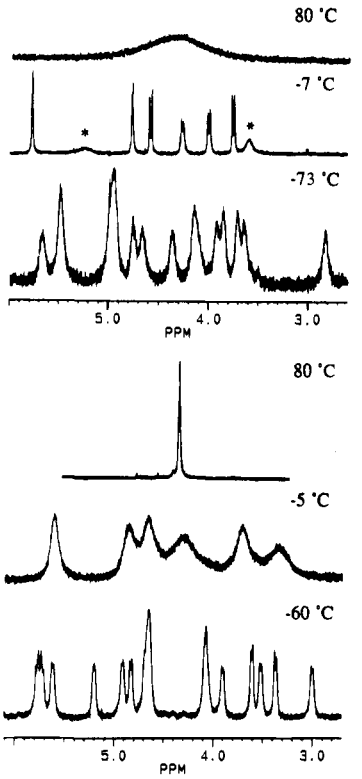

Figure 5. ^{1}H NMR spectra ($-CH_2-$ region) for $M_2(OCH_2{}^tBu)_8(py)$ complexes in toluene-d_8 as a function of temperature. Top three spectra, M = Mo; bottom three spectra, M = W. Note: A ^{1}H–^{1}H COSY spectrum of $Mo_2(OCH_2{}^tBu)_8(py)$ at −7 °C conclusively established that the broad resonances denoted with an asterisk (second spectrum from the top) were coupled.

that could yield laddered structures or in the simplest case the one-dimensional polymer shown in **VII**.

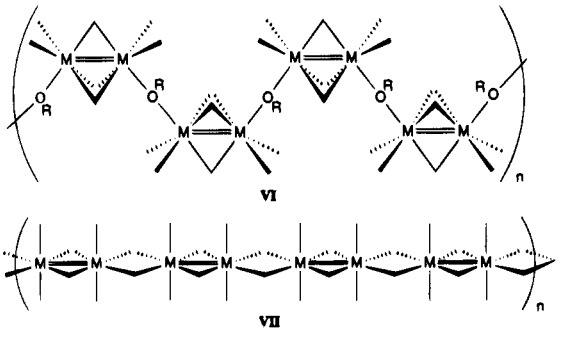

VI

VII

As was previously stated the addition of pyridine to toluene suspensions of $W_2(OCH_2{}^tBu)_8$ and $Mo_2(OCH_2{}^tBu)_8$ results in the formation of homogeneous solutions. Based on titration experiments as well as integration of the ^{1}H NMR spectra the solutions contain $M_2(OCH_2{}^tBu)_8(py)$ complexes which are fluxional at room temperature. At intermediate temperatures the fluxionality is relatively slow compared to the time scale of ^{1}H NMR spectroscopy and the spectra are consistent with a confacial bioctahedral arrangement of ligands with a terminally bound pyridine.

Remarkably, as the solutions are cooled further the spectra become extremely complex (Figure 5) until at very low temperatures (−65 °C, M = W, and −78 °C, M = Mo) they are consistent with C_1 symmetry for the $M_2(OCH_2{}^tBu)_8(py)$ formula unit. This second process is independent of the concentration of metal complex or pyridine and by integration it is quite clear that a single molecule of this donor ligand is bound per $M_2(OCH_2{}^tBu)_8$ at very low temperatures. These observations rule out the possibility that increased aggregation

(18) Chisholm, M. H.; Reichert, W. W.; Thornton, P. *J. Am. Chem. Soc.* **1978**, *100*, 2744.
(19) Chisholm, M. H.; Huffman, J. C.; Ratermann, A. L.; Smith, C. A. *Inorg. Chem.* **1984**, *23*, 1596.

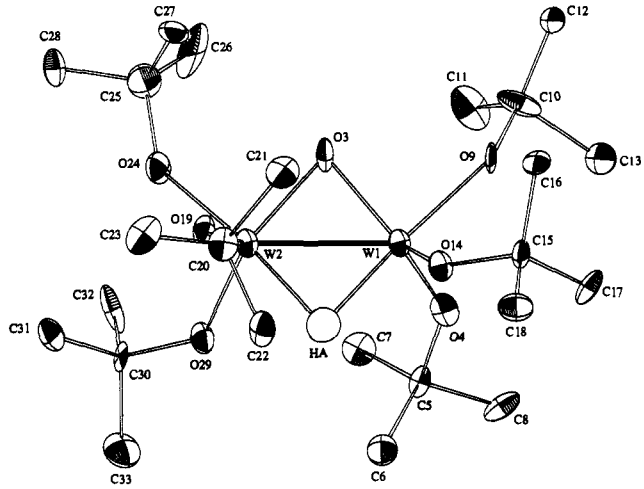

Figure 6. An ORTEP drawing of the counter-cation (η^6-18-crown-6)K$^+$(μ-η^2,η^2-18-crown-6)K$^+$(η^6-18-crown-6) which resides at a crystallographic inversion center. Ellipsoids are shown at the 30% probability level, and hydrogen atoms have been omitted for clarity.

Table 4. Pertinent Bond Distances and Angles for [K(18-crown-6)$_{1.5}$]$^+$[W$_2$(μ-H)(μ-O)(O^{t}Bu)$_6$]$^-$

	Distances (Å)		
W(1)−W(2)	2.445(1)	W(2)−O(3)	1.932(11)
W(1)−O(3)	1.916(12)	W(2)−O(19)	1.881(10)
W(1)−O(4)	1.888(12)	W(2)−O(24)	2.025(12)
W(1)−O(9)	2.013(11)	W(2)−O(29)	1.938(11)
W(1)−O(14)	1.953(10)	K−O(av)	2.859(13)
	Angles (deg)		
W(1)−W(2)−O(3)	50.3(3)	W(2)−W(1)−O(3)	50.9(3)
W(1)−W(2)−O(19)	111.4(3)	W(2)−W(1)−O(4)	112.5(4)
W(1)−W(2)−O(24)	135.2(3)	W(2)−W(1)−O(9)	136.5(3)
W(1)−W(2)−O(29)	111.6(3)	W(2)−W(1)−O(14)	109.8(3)
O(3)−W(1)−O(4)	116.8(5)	O(3)−W(2)−O(19)	113.6(5)
O(3)−W(1)−O(9)	85.8(4)	O(3)−W(2)−O(24)	85.7(5)
O(3)−W(1)−O(14)	126.7(5)	O(3)−W(2)−O(29)	131.1(5)
O(4)−W(1)−O(9)	88.8(5)	O(19)−W(2)−O(24)	92.0(5)
O(4)−W(1)−O(14)	116.3(5)	O(19)−W(2)−O(29)	115.3(5)
O(9)−W(1)−O(14)	91.6(4)	O(24)−W(2)−O(29)	89.8(5)
W(1)−O(3)−W(2)	78.9(5)		

is responsible for the spectroscopic changes. Plausible low-temperature structures which explain this behavior are not readily apparent, but we remain hopeful to resolve this issue by single-crystal X-ray diffraction.

Thermal Decomposition of [W$_2$(O^{t}Bu)$_7$]$^-$ to [W(μ-H)(μ-O)(O^{t}Bu)$_6$]$^-$ and Isobutylene. In contrast to [Mo$_2$(O^{t}Bu)$_7$]$^-$ ions that are thermally persistent in solution, showing only evidence of reversible dissociation of [O^{t}Bu]$^-$, the [W$_2$(O^{t}Bu)$_7$]$^-$ anion cleanly decomposes (is transformed) to the hydrido−oxo ditungsten anion [W$_2$(μ-H)(μ-O)(O^{t}Bu)$_6$]$^-$ with the liberation of isobutylene.

The anion has been crystallographically characterized as a salt with the counter cation (η^6-18-crown-6)K$^+$(μ-η^2,η^2-18-crown-6)K$^+$(η^6-18-crown-6) which in the space group $P2_1/n$ resides on a crystallographic inversion center. A view of the molecule is shown in Figure 6 and selected bond, distances and angles are reported in Table 4.

The hydride ligand which was not crystallographically located is placed in a bridging position in the plane of the W$_2$(μ-O) moiety. This position is acceptable to the hydride-locating program of Orpen, XHYDEX,[20] and is consistent with the ^{1}H NMR data that reveal a hydride signal flanked by ^{183}W satellites of *ca.* 26% intensity (see Experimental Section). The geometry of the anion can be described in terms of two trigonal bipyramids fused along a common equatorial (μ-O) and axial (μ-H) site.

(20) Orpen, A. G. *J. Chem. Soc., Dalton Trans.* **1980**, 2509.

The W−W distance of 2.445(1) Å is consistent with the presence of a (W=W)$^{8+}$ moiety. The W−O^{t}Bu distances trans to the μ-H ligand are larger than those in the equatorial plane by *ca.* 0.10 Å. By ^{1}H NMR spectroscopy we observe only one type of O^{t}Bu ligand indicating that axial ⇌ equatorial site exchange is rapid on the NMR time scale. The W−μ-O distances of 1.92(1) Å (av) rule out the possibility of a bridging hydroxide group which would, like μ-OR ligands, have a W−O distance of 2.0−2.10 Å. Moreover, there is no evidence of ν-(O−H) at >3000 cm^{-1} in the IR spectrum. There is therefore no question that this anion is an hydrido−oxo tungsten complex of formula [W$_2$(μ-H)(μ-O)(O^{t}Bu)$_6$]$^-$.[21]

It should be emphasized that the decomposition of [K(18-crown-6)]$^+$[W$_2$(O^{t}Bu)$_7$]$^-$ occurs at room temperature in solution and even in the solid state.

The direct observation of the decomposition of an alkoxide ligand within a metal complex is rare. For late transition metal complexes the evidence gathered thus far indicates that the preponderant pathway for alkoxide decomposition involves facile β-hydride elimination.[22] Only in the case of copper alkoxide complexes has a radical pathway been implicated, but even then decomposition by β-hydride elimination was a competitive reaction.[22d] For earlier members of the transition series, β-hydride elimination from alkoxide ligands is not favorable (the microscopic reverse, insertion of a ketone or aldehyde into an M−H bond, is) but clearly implicated in the racemization of chiral secondary alcohols by metal alkoxide complexes of niobium, tantalum, and more recently rhenium.[23] An energetic balance is reached in the middle of the transition series as shown by Hoffman *et al.* in their report concerning the facile and reversible equilibrium between Re$_3$(O^{i}Pr)$_{12}$ and Re$_3$(H)(O^{i}Pr)$_{11}$.[24]

Tertiary alkoxide ligands are incapable of this reaction but may decompose by net γ-CH activation.[25a] The latter process allows the deposition of CuO at 510 K from [Cu(O^{t}Bu)]$_4$ by MOCVD.[25b] Alternatively, trace acid may catalyze the dehydration of tertiary alkoxide ligands as was demonstrated by Bradley and Faktor for Zr(O^{t}Amyl)$_4$.[26]

In one instance the decomposition of a metal alkoxide was shown to proceed via alkyl migration to give an oxo−alkyl complex.[27] The latter represents a net oxidation of the metal: M−OR → M(=O)(R), and, superficially at least, is similar to the process described here: M−OR → M(=O)(H). We hasten to add, however, that the alkyl migration proceeded only at elevated temperatures with a rather high activation barrier ($\Delta G^\ddagger$ = 34.5 kcal/mol), in contrast to the facile γ-CH activation reaction exhibited by [W$_2$(O^{t}Bu)$_7$]$^-$.

(21) The structural differences which occur upon μ-OH ⇌ μ-O change have been addressed. See for instance: Cotton, F. A.; Diebold, M. P.; Roth, W. J. *Inorg. Chim. Acta* **1988**, *149*, 105.

(22) (a) Bryndza, H. E.; Tam, W. *Chem. Rev.* **1988**, *88*, 1163. (b) Bryndza, H. E.; Calabreses, J. C.; Marsi, M.; Roe, D. C.; Tam, W.; Bercaw, J. E. *J. Am. Chem. Soc.* **1986**, *108*, 4805. (c) Bernard, K. A.; Rees, W. M.; Atwood, J. D. *Organometallics* **1986**, *5*, 390. (d) Whitesides, G. M.; Sadowski, J. S.; Lilburn, J. *J. Am. Chem. Soc.* **1974**, *96*, 2829.

(23) (a) Nugent, W. A.; Zubyk, R. M. *Inorg. Chem.* **1986**, *25*, 4604. (b) Saura-Llamas, I.; Gladysz, J. A. *J. Am. Chem. Soc.* **1992**, *114*, 2136.

(24) Hoffman, D. M.; Lappas, D.; Wierda, D. A. *J. Am. Chem. Soc.* **1993**, *115*, 10538.

(25) (a) Brainard, R. L.; Madix, R. J. *Surf. Sci.* **1989**, *214*, 396. (b) Jeffries, P. M.; Dubois, L. H.; Girolami, G. S. *Chem. Mater.* **1992**, *4*, 1169.

(26) (a) Bradley, D. C.; Faktor, M. M. *J. Am. Chem. Soc.* **1959**, *9*, 435. (b) Bradley, D. C.; Faktor, M. M. *J. Chem. Soc., Faraday Trans.* **1959**, *55*, 2117.

(27) (a) Cp$_2$*Ta(η^2-O=CH$_2$)(H) thermally rearranges to Cp$_2$*Ta(=O)(CH$_3$) by way of the alkoxide intermediate Cp$_2$*Ta(OCH$_3$). Without thermodynamic data for all three, estimation of the relative contribution of the alkoxide decomposition process to the overall barrier of the reaction is impossible. See: (b) Parkin, G.; Burnel, E.; Burger, B. J.; Trimmer, M. S.; van Asselt, A.; Bercaw, J. E. *J. Mol. Catal.* **1987**, *41*, 21.

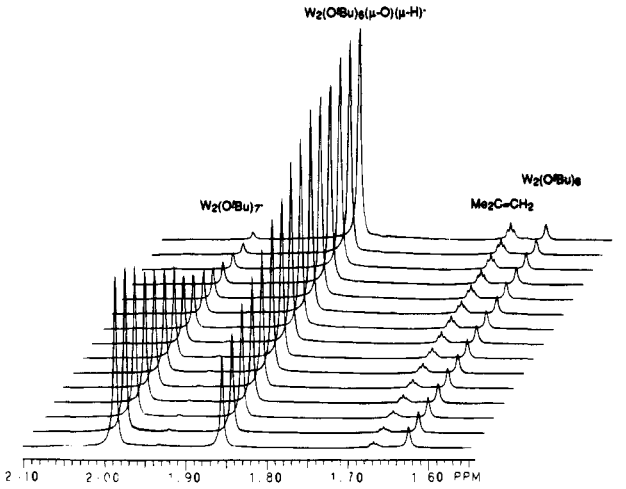

Figure 7. Stacked plot of ^{1}H NMR spectra at 61 °C showing the decomposition of **2a** to $[W_2(\mu\text{-H})(\mu\text{-O})(O^tBu)_6]^-$ in the presence of $W_2(O^tBu)_6$. The time scale from the first to last spectrum is 3400 s. Note that the sharp lines observed for each of the tungsten-containing species indicate that exchange of ^{t}BuO− ligands among these complexes is slow relative to the NMR time scale.

We have studied the rate of the reaction shown in eq 4 by ^{1}H NMR spectroscopy in pyridine-d_5 as a function of temperature (23−80 °C), with and without added KO^{t}Bu (see Figure 7). In the temperature range studied there is little dissociation to give $W_2(O^tBu)_6$ and we found that the rate was first order in

$$[W_2(O^tBu)_7]^- \xrightarrow[\text{pyridine-}d_5]{T\,^\circ C} [W_2(\mu\text{-H})(\mu\text{-O})(O^tBu)_6]^- + Me_2C{=}CH_2 \quad (4)$$

$[W_2(O^tBu)_7]^-$ and independent of [KO^{t}Bu]. The activation parameters were determined from an Eyring plot yielding $\Delta H^\ddagger = 23.1(5)$ kcal/mol and $\Delta S^\ddagger = -3.3(5)$ eu.

Since this is the sole example of the decomposition of an alkoxide ligand to give a metal hydrido−oxo-containing complex we were interested in investigating further aspects of the mechanism by performing deuterium isotopic substitution reactions.

First, in the decomposition of the perdeuterio anion $[W_2(OC(CD_3)_3)_7]^-$ the product is $[W_2(\mu\text{-D})(\mu\text{-O})(O^tBu\text{-}d_9)_6]^-$ and the μ-deuteride does not exchange with the hydroxyl proton of ^{t}BuOH once formed. [The ^{t}BuOH for d_9-^{t}BuOH exchange on the ditungsten center does occur, presumably by the normal route for alcohol/alkoxide exchange.[8]] The rate of reaction 4 showed a marked kinetic isotope effect $k_H/k_D = 3.5(1)$ at 23 °C which implies that carbon−hydrogen bond breaking contributes significantly to the overall rate of the reaction. We also prepared the partially deuterated complex anion $[W_2(OC(CH_3)(CD_3)_2)_7]^-$, in order to measure the intramolecular isotope effect which is an absolute measure of the facility for breaking C−H versus C−D bonds. C−H bond rupture would yield $(CD_3)_2C{=}CH_2$ while C−D bond rupture generates $(CH_3)(CD_3)C{=}CD_2$. The observed isotope effect k_H/k_D determined in this manner was 3.5(4) which is, within the limits of experimental error, identical to that determined from a comparison of the rates of decomposition, eq 4, for the all protio versus the all deuterio complex anion. This leads us to conclude that carbon−hydrogen bond breaking is involved in the activated complex.

We are struck by the fact that this reaction occurs for the $[W_2(O^tBu)_7]^-$ anion and not for the molybdenum analogue. Reaction 4 represents an oxidation of the $(M{\equiv}M)^{6+}$ center to $(M{=}M)^{8+}$ and this is well-known now to occur more readily for M = W than M = Mo.[28] Moreover, if we replace one methyl group by a trifluoromethyl group we observed that the complex anion $[W_2(OCMe_2(CF_3))_7]^-$ is formed but does not decompose under the same conditions to give $[W_2(\mu\text{-H})(\mu\text{-O})(OCMe_2(CF_3)_6]^-$. Thus, we propose that the facility of the reaction shown in eq 4 rests with the ease of oxidation of the metal center. Note, although $W_2(O^tBu)_6$ is not thermally persistent in solution at temperatures above 90 °C its decomposition is notably slower than that of the electron rich anion $[W_2(O^tBu)_7]^-$.

Table 5. Rate Data for the Thermal Decomposition of $[W_2(O^tBu)_7]^-$ and $[W_2(O^iPr)_7]^-$

T (°C)	anion	k_{obs} (s^{-1})	T (°C)	anion	k_{obs} (s^{-1})
22.8	$[W_2(O^tBu)_7]^-$	9.08×10^{-6}			
37.2	$[W_2(O^tBu)_7]^-$	6.48×10^{-5}	40.2	$[W_2(O^iPr)_7]^-$	2.22×10^{-5}
44.3	$[W_2(O^tBu)_7]^-$	1.54×10^{-4}	50.3[a]	$[W_2(O^iPr)_7]^-$	7.95×10^{-5}
50.3	$[W_2(O^tBu)_7]^-$	2.96×10^{-4}	50.3	$[W_2(O^iPr)_7]^-$	7.21×10^{-5}
50.3[a]	$[W_2(O^tBu)_7]^-$	2.86×10^{-4}	60.5	$[W_2(O^iPr)_7]^-$	2.52×10^{-4}
60.6	$[W_2(O^tBu)_7]^-$	9.61×10^{-4}	70.6	$[W_2(O^iPr)_7]^-$	6.28×10^{-4}
70.6	$[W_2(O^tBu)_7]^-$	2.21×10^{-3}	80.9	$[W_2(O^iPr)_7]^-$	1.69×10^{-3}
80.7	$[W_2(O^tBu)_7]^-$	7.68×10^{-3}	91.0	$[W_2(O^iPr)_7]^-$	6.19×10^{-3}

[a] Reaction conducted in the presence of [KOR] = 7×10^{-2} M (~1 equiv).

The decomposition of $[W_2(O^iPr)_7]^-$ proceeds in a similar manner to yield the hydrido−oxo anion $[W_2(\mu\text{-H})(\mu\text{-O})(O^iPr)_6]^-$ and propene as shown in eq 5.

$$[W_2(O^iPr)_7]^- \xrightarrow{C_5D_5N} [W_2(\mu\text{-H})(\mu\text{-O})(O^iPr)_6]^- + \text{propene} \quad (5)$$

At elevated temperatures the spectroscopic properties of this hydrido−oxo anion are very similar to those of the analogous *tert*-butoxide complex. A single set of alkoxide resonances is observed, and the hydride signal occurs at δ 7.10 ppm with J_{W-H} = 130 Hz (26%). At lower temperatures association of pyridine occurs on the NMR time scale and the spectra are more complex. For this process the measured rates (40−90 °C) are ~4 times slower than those observed for the decomposition of **2a** (Table 5). The activation parameters are, however, very similar: $\Delta H^\ddagger = 23.8(8)$ kcal/mol, $\Delta S^\ddagger = -4(2)$ eu. We conclude that the same mechanism is operative for both eqs 4 and 5, and that eq 4 is faster due to the greater e$^-$-donating power of a *tert*-butoxide ligand (compared to isopropoxide) and the greater number of γ-C−H bonds present in **2a** compared to **2b**.

It has been said that kinetics is to mechanism as science is to fiction.[29] Nevertheless, one carries out kinetics and other mechanistic studies with the purpose of gaining insight into reaction pathways and obtaining the privilege of scientific speculation. Within this context we are drawn to the parallel that can be made with the retro-ene reaction shown in Scheme 1. In this reaction pathway, there is a cyclic transition state and the metal is oxidized as the isobutylene is formed (eliminated). This accounts nicely for both the metal dependence (ease of oxidation) and the observed kinetic isotope effect.

At this point it is impossible to identify conclusively the exact location of H-atom transfer, which may proceed to the metal via an alkoxide oxygen: if through the oxygen of the same alkoxide ligand then the intermediate is a hydroxide complex which tautomerizes to the observed hydrido−oxo species, and if through the oxygen atom of a different alkoxide ligand then the intermediate contains a coordinated alcohol which oxidatively adds to the $(W{\equiv}W)^{6+}$ center to provide the final product. Both of these possibilities are well-precedented in the literature.[30]

(28) Chisholm, M. H. *Polyhedron* **1986**, *5*, 25.
(29) Attributed to the late Professor R. S. Nyholm.

Scheme 1

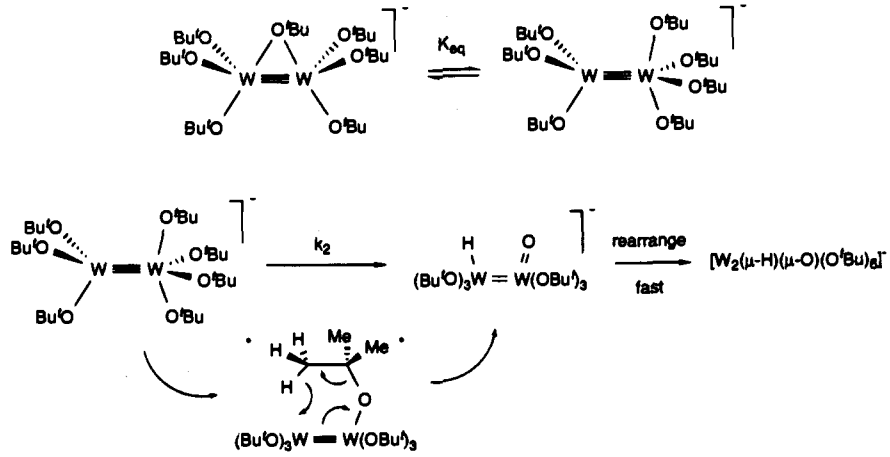

Scheme 2

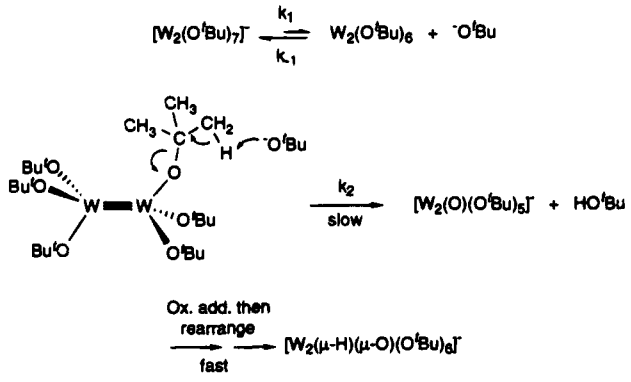

With regards to the observed $\Delta S^{\ddagger}$ for the overall transformation, it is somewhat larger than is typically observed for retro-ene reactions which proceed with $\Delta S^{\ddagger}$ in the range -5 to -15 eu.[31] However, another factor that cannot be ignored is the proposed rapid pre-equilibrium involving bridge-to-terminal migration of an alkoxide ligand as shown in Scheme 1. The observed rate constant would manifest contributions of this migration in $\Delta H^{\ddagger}$ and $\Delta S^{\ddagger}$ for the overall reaction since $k_{obs} = K_{eq}k_2$. The pre-equilibrium would be entropically favorable and this would then account for the larger than expected observed value for $\Delta S^{\ddagger}$. Given the fluxionality of the complex anion $[W_2(O^tBu)_7]^-$ the proposed coordination geometry should be easily accessible. For the bulky O^{t}Bu ligand K_{eq} would be larger than that for O^{i}Pr and this could contribute to the observed rates of decomposition of **2a** relative to **2b**.

Finally one other point needs consideration. The first-order dependence of reaction 4 on $[W_2(O^tBu)_7]^-$ and the independence of this reaction on [KO^{t}Bu] do not preclude a bimolecular decomposition pathway. On the contrary, a pathway involving dissociation of $^-$O^{t}Bu from $W_2(O^tBu)_7^-$ followed by deprotonation of $W_2(O^tBu)_6$ by $^-$O^{t}Bu and subsequent rapid oxidative addition of HO^{t}Bu is also consistent with the observed kinetics. For this scenario $k_{obs} = k_1k_2/(k_{-1} + k_2)$ as shown in Scheme 2. A crossover experiment was devised to distinguish between these possibilities which made use of the chemical inertness of the μ-H ligand once it is formed. The decomposition of $[W_2(O^tBu)_7]^-$ was carried out in pyridine in the presence of a large excess of DO^{t}Bu. If the pathway shown in Scheme 2 was operative then a significant (if not complete) percentage of the product should be deuterated. Instead no incorporation of deuterium was observed and the product was exclusively $[W_2(\mu\text{-H})(\mu\text{-O})(O^tBu)_6]^-$ as shown in eq 6. This is consistent

$$[W_2(O^tBu)_7]^- + 100DO^tBu \xrightarrow[C_5D_5N]{65\ ^\circ C} [W_2(\mu\text{-H})(\mu\text{-O})(O^tBu)_6]^- + Me_2C{=}CH_2 \quad (6)$$

with the pathway in Scheme 1 and any other intramolecular pathway that does not involve the formation of long-lived intermediates containing exchangeable (*i.e.* acidic) protons. So, for instance, this rules out a solvent-assisted pathway involving the formation of pyridinium cations and suggests that H-atom transfer occurs directly to the metal and not via alkoxide oxygen as was discussed previously.

We have also attempted the deprotonation of $W_2(O^tBu)_6$ with the extremely bulky bases $^-OC(^tBu)_3$ and $^-OSi(^tBu)_3$ wherein steric pressure prevents the formation of complex anions such as $[W_2(O^tBu)_6(OC^tBu_3)]^-$ and $[W_2(O^tBu)_6(OSi^tBu_3)]^-$. In neither case was any significant reaction observed even after heating at 65 °C in C_5D_5N for 2 h.

The complex anion $[W_2(\mu\text{-H})(\mu\text{-O})(O^tBu)_6]^-$ is not preparable in high yield from KOH and $W_2(O^tBu)_6$ in THF or pyridine in the presence of 18-crown-6. Instead only a low yield of this species (*ca.* 30%) is found in the product mixture. In contrast KOH reacts with 2 equiv of $Mo_2(OCH_2{}^tBu)_6$ in THF/18-crown-6 to form $[Mo_4(\mu_3\text{-O})(OCH_2{}^tBu)_{11}]^-[K(18\text{-crown-6})]^+$ in greater than 90% isolated crystalline yield.[32] Note that the molybdenum-containing product is not oxidized, and any intermediate complex hydroxide anion such as $[Mo_2(OH)(OCH_2{}^tBu)_6]^-$ reacts with another equivalent of $Mo_2(OCH_2{}^tBu)_6$ and liberates an equivalent of $HOCH_2{}^tBu$ rather than tautomerizing to form a μ-hydrido μ-oxo species.

Reactions with Carbon Monoxide. The additional alkoxide donor ligands present in the complex anions **2a**–**e**, **3b**, and **3e** clearly affect the energetics of the M_2^{6+} moiety as evidenced by the electronic spectra which show bands that are red-shifted relative to the neutral $M_2(OR)_6$ compounds. This alteration of the $(M{\equiv}M)^{6+}$ bonding energies is manifested in the reactivity of the dianions **3b** and **3e** with Ph_3PBr_2 as well as the thermal lability of **2a** and **2b** (eqs 4 and 5). We were therefore interested in probing the reaction of carbon monoxide with these anions. (The $M_2(OR)_6$ complexes themselves react with CO to form 1:1 adducts that exhibit substantially reduced C≡O bonds.[33]

(30) (a) M–OH ⇌ M(H)(O): Tahmassebi, S. K.; Conry, R. R.; Mayer, J. M. *J. Am. Chem. Soc.* **1993**, *112*, 8600. (b) van Asselt, A.; Burger, B. J.; Gibson, V. C.; Bercaw, J. E. *J. Am. Chem. Soc.* **1986**, *108*, 5347. (c) $W_2(O^iPr)_6 + HO^iPr \rightarrow W_2(H)(O^iPr)_7$: Chisholm, M. H.; Huffman, J. C.; Smith, C. A. *J. Am. Chem. Soc.* **1986**, *108*, 222.

(31) (a) Hoffmann, H. M. R. *Angew. Chem., Int. Ed. Engl.* **1969**, *8*, 556. (b) Oppolzer, W.; Snieckus, V. *Angew. Chem., Int. Ed. Engl.* **1978**, *17*, 476.

(32) Budzichowski, T. A.; Chisholm, M. H.; Folting, K. Results to be submitted for publication.

Further addition of CO may lead to $W(CO)_6$ and products derived from cleavage of the W≡W bond.)

Our preliminary results suggest that there is reaction between the monoanions and CO, but this is limited to simple adduct formations as shown in eq 7. The products are characterized

$$[M_2(OR)_7]^- + CO \xrightarrow{C_5D_5N} [M_2(OR)_7(CO)]^- \qquad (7)$$

by their δ ^{13}CO chemical shifts which occur in the range 220–260 ppm and are not indicative of cleavage of the CO bond.[34] The ν(CO) for these complexes occur at 1595–1640 cm^{-1} which shows that the CO ligand is significantly reduced.

In contrast, the dianions **3b** and **3e** do not react with CO, presumably due to steric factors that prevent CO access to the electron-rich M_2^{6+} center. Even after prolonged heating at 65 °C in THF-d_8, little, if any, reaction is observed between **3b** and CO.

Concluding Remarks

The $M_2(OR)_6$ compounds are coordinatively unsaturated and π-buffered. Their Lewis acidity is also influenced by steric factors associated with R. We have found that in hydrocarbon solvents they are inert with respect to nucleophilic uptake of halide ions and pseudo-halide NCS^- which could, of course, bind via the hard nitrogen or soft sulfur. With cyanide anion, which is also a pseudo-halogen but is a stronger base, there is a reversible equilibrium involving the formation of $[M_2(OR)_6(CN)]^-$ and $[M_2(OR)_8(CN)_2]^{2-}$ anions. In this work we have found that the $M_2(OR)_6$ complexes will react with KOR to form $[M_2(OR)_7]^-$ and $[M_2(OR)_8]^{2-}$ anions and that the preference for the coordination of OR^- follows the trend M = W and R = $CH_2{}^tBu$ > ^iPr > ^tBu in parallel with that seen for CN^- binding. The structure of the $[M_2(OR)_7]^-$ anions, as determined for M = Mo and R = $CH_2{}^tBu$, represents a new structural type for so-called d^3–d^3 dimers of molybdenum and tungsten.[4] The fluxional behavior of these monoanions is an indication of the rapid opening and closing of OR bridges and probably provides a clue as to the mechanism of scrambling in the reactions involving 1,2-$Mo_2Br_2(CH_2SiMe_3)_4$ and Me_2NH (>2 equiv) and $LiNMe_2$ (2 equiv) which lead to 1,2-$Mo_2(NMe_2)_2(CH_2SiMe_2)_4$ and 1,1-$Mo_2(NMe_2)_2(CH_2SiMe_3)_4$, respectively.[35] The monobridged structure of the $[M_2(OR)_7]^-$ anions contrasts with the structures seen for $Mo_2(CH_2Ph)_2(O^iPr)_4(PMe_3)$ and W_2(p-tolyl)$_2(O^iPr)_4(HNMe_2)$ that have unbridged M≡M bonds involving 3- and 4-coordinated metal atoms.[36] Charge balance between the metal centers presumably favors the bridged structure for the anion. The pyramidal oxygen of the μ-OR ligand is also a point of note and extremely rare in metal alkoxide chemistry. This is readily understood on electronic grounds as noted in the orbital interactions shown in **III** and **IV**. The dianions $[M_2(OR)_8]^{2-}$ have an eclipsed $O_4M{\equiv}MO_4$ core as a result of the binding of the potassium ions to opposite faces of the O_8 cube. The $[W_2(OCH_2{}^tBu)_8]^{2-}$ dianion provides a useful entry point for the formation of $W_2(OCH_2{}^tBu)_8$ that has not previously been accessible. The thermal decomposition of $[W_2(OR)_7]^-$ anions provides rare insight into the selective intramolecular activation of alkoxide ligands. The formation of the $[W_2(\mu\text{-H})(\mu\text{-O})(OR)_6]^-$ anions represents oxidation to the W_2^{8+} center and this we feel is due to the increased electron density and higher M–M orbital energy of the $[M_2(OR)_7]^-$ anions. This point is further emphasized by the comparative values of $\bar{\nu}$(CO) in $Mo_2(O^tBu)_6(CO)$[33a] and $[Mo_2(O^tBu)_7(CO)]^-$ that occut at 1670 and 1637 cm^{-1}, respectively. It also should be remembered that while $W_2(O^tBu)_6$ and an excess of ^iPrOH yield only $W_2(^iOPr)_6$ (and its dimer $W_4(O^iPr)_{12}$)[6] in the presence of base such as NaO^iPr oxidative addition occurs to yield the $[W_2(H)(O^iPr)_8]^-$ anion.[30c] Furthermore, the thermal sensitivity of the $[W_2(O^iPr)_7]^-$ anion and its facile formation of $[W_2(O)(H)(O^iPr)_6]^-$ underscore the fact that steric factors alone are not operative. The facility of the decomposition of the $[M_2(OR)_7]^-$ anions is clearly rooted in the differences in the reactivities of the $(M{\equiv}M)^{6+}$ moieties W *vs* Mo and attests to the greater ease of oxidation of the ditungsten centers.[37] Note in this regard that the introduction of the $-OCMe_2(CF_3)$ ligand which is less electron donating suppresses this decomposition.

Experimental Section

All synthetic procedures were performed under an inert atmosphere utilizing standard procedures in conjunction with a Vacuum Atmospheres Corporation Dri-Lab. The solvents used were dried by standard procedures and stored over 4 Å molecular sieves. Benzene-d_6, toluene-d_8, methylene dichloride-d_2, pyridine-d_5, and ^tBuOH-d_9 were obtained commercially but were degassed and stored over 4 Å molecular sieves prior to use. The metal alkoxides were prepared as described in the literature[7a,9] and were recrystallized from cold hexanes and dried *in vacuo* prior to use. Ph_3PBr_2 was used as supplied from a commercial source (Aldrich). The crown ether (18-crown-6) was purchased from Aldrich and was purified by repeated sublimation (100 °C, 0.001 Torr) prior to use. ^tBuOH-d_6 was prepared from MeMgBr and acetone-d_6 in diethyl ether, purified by distillation, and dried over 4 Å molecular sieves. The potassium alkoxides used were prepared from potassium metal and the appropriate alcohol in THF and were dried (80 °C, 0.01 Torr) prior to use with the exception of KO^tBu which was sublimed (100 °C, 0.01 Torr). NMR spectra were recorded on Varian XL-300 (300.1 MHz) and Bruker AM-500 (500.0 MHz) spectrometers and were referenced to residual protio impurities of the deuterated solvents. Thermodynamic and kinetic measurements were performed on the former with temperature calibrated using a sample of neat ethylene glycol and the program Temcal(E).[38] The data were analyzed according to standard procedures.[39] Infrared spectra were recorded on a Nicolet 510P FT-IR spectrometer. UV–visible spectra were recorded in THF on a Hewlett-Packard 8452A diode array spectrophotometer.

Synthesis of Monoanion Complexes 2d–f. Equimolar amounts of the appropriate $Mo_2(OR)_6$ complex (0.915 mmol), crown ether (1.1 eq), and potassium alkoxide were weighed into a Schlenk flask in a nitrogen-filled glovebox. THF (~10 mL) was then added outside the box with the aid of a cannula and the resulting solution was stirred for 1 h. The solvent was then removed *in vacuo* (23 °C, 0.01 Torr) and the residue recrystallized from hot C_6H_6 (R = $CH_2{}^tBu$) or THF/hexanes at −65 °C (R = ^tBu, ^iPr). The crystalline material was then isolated by filtration and washed with hexanes or cold (−65 °C) toluene. The isolated yields are 82% of **2d**, 85% of **2e**, and 91% of **2f**, respectively. For $[K(18\text{-crown-6})]^+[Mo_2(O^tBu)_7]^-$ (**2d**): ^1H NMR (C_5D_5N, 300 MHz, 23 °C) δ 3.50 (s, 24H), 1.97 (s, 63H). $^{13}C\{^1H\}$ NMR (C_5D_5N, 75

(33) (a) Chisholm, M. H.; Cotton, F. A.; Extine, M. H.; Kelly, R. H. *J. Am. Chem. Soc.* **1979**, *101*, 7645. (b) Chisholm, M. H.; Huffman, J. C.; Leonelli, J.; Rothwell, I. P. *J. Am. Chem. Soc.* **1982**, *104*, 7030. (c) Chisholm, M. H.; Hoffman, D. M.; Huffman, J. C. *Organometallics* **1985**, *4*, 986. (d) Blower, P. J.; Chisholm, M. H.; Clark, D. L.; Eichhorn, B. W. *Organometallics* **1986**, *5*, 2125.

(34) The reaction between CO and 1,2-$W_2Cl_2(silox)_4$ where silox = $^tBu_3SiO$ leads to a μ-carbido terminal oxo compound by cleavage of C≡O, $W_2(\mu\text{-C})(O)Cl_2(silox)_4$: Miller, P. L.; Wolczanski, P. T.; Rheingold, A. L. *J. Am. Chem. Soc.* **1993**, *115*, 10422.

(35) Chisholm, M. H.; Folting, K.; Huffman, J. C.; Rothwell, I. P. *Organometallics* **1982**, *1*, 251.

(36) (a) Chisholm, M. H.; Huffman, J. C.; Tatz, R. J. *J. Am. Chem. Soc.* **1984**, *106*, 5385. (b) Chisholm, M. H.; Folting, K.; Huffman, J. C.; Kramer, K. S.; Tatz, R. J. *Organometallics* **1992**, *11*, 4029. (c) Chisholm, M. H.; Eichhorn, B. W.; Folting, K.; Huffman, J. C.; Tatz, R. J. *Organometallics* **1986**, *5*, 1599.

(37) A comparison of the ease of oxidative-addition to and reductive-elimination from $(M{\equiv}M)^{6+}$ centers is presented in ref 22. The difference in oxidation potentials of related $(M\overset{4}{-}M)^{4+}$ and $(M\overset{3}{-}M)^{6+}$ complexes can be measured by cyclic voltammetry or photoelectron spectroscopy and is *ca.* 0.5 V or 0.5 eV, respectively. See: Lichtenberger, D. L.; Johnston, R. L. In *Metal–Metal Bonds and Clusters in Catalysis*; Fackler, J. P., Ed.; Plenum Press: New York and London, 1990; p 275.

(38) Patt, S. *XL-Series Basic Operation Manual*; Publication No. 87-146-054; Varian Instrument Division: Palo Alto, 1985.

(39) Espenson, J. H. *Chemical Kinetics and Reaction Mechanisms*; McGraw-Hill: New York, 1981.

MHz, 23 °C) δ 76.83 ($-OCMe_3$), 70.39 ($-OCH_2CH_2-$), 34.84 ($-OC(CH_3)_3$). IR (KBr pellet, cm^{-1}) 2961 s, 2913 s, 1473 w, 1465 w, 1352 s, 1225 m, 1182 s, 1109 s, 964 s, 958 s, 837 w, 770 w, 567 w. UV−vis (THF, nm) 210 (ϵ = 17000), 252 (ϵ = 8200), 294 sh (ϵ = 3000), 384 (ϵ = 590), 550 v br (ϵ = 175). Anal. Calcd for $C_{40}H_{87}KMo_2O_{13}$: C, 47.71; H, 8.70. Found: C, 47.41; H, 8.73. For $[K(18\text{-crown-}6)]^+[Mo_2(O^iPr)_7]^-$ (**2e**): ^1H NMR (C_6D_6, 500 MHz, 23 °C) δ 5.79 (hept, 7H), 3.10 (s, 24H), 1.69 (d, 42H). $^{13}C\{^1H\}$ NMR (C_6D_6, 125 MHz, 23 °C) δ 69.98 ($-OCH_2CH_2-$), 69.55 ($-OCHMe_2$), 28.38 ($-OCH(CH_3)_2$). IR (KBr pellet, cm^{-1}) 2957 s, 2909 s, 1462 w, 1354 m, 1319 w, 1251 w, 1115 br s, 972 br s, 964 s, 835 br m, 617 m, 588 w, 430 w. UV−vis (THF, nm) 222 (ϵ = 3300), 258 (ϵ = 3600), 292 sh (ϵ = 3300), 370 (ϵ = 1250), 540 v br (ϵ = 390). Anal. Calcd for $C_{33}H_{73}KMo_2O_{13}$: C, 43.61; H, 8.09. Found: C, 43.22; H, 8.00. For $K(18\text{-crown-}6)]^+[Mo_2(OCH_2{}^tBu)_7]^-$ (**2f**): ^1H NMR (C_5D_5N, 500 MHz, 23 °C) δ 4.70 (s, 14H), 3.46 (s, 24H), 1.32 (s, 63H). $^{13}C\{^1H\}$ NMR (C_5D_5N, 125 MHz, 23 °C) δ 81.55 ($-OCH_2{}^tBu$), 70.42 ($-OCH_2CH_2-$), 34.67 ($-OCH_2CMe_3$), 28.10 ($-OCH_2C(CH_3)_3$). IR (KBr pellet, cm^{-1}) 2945 s, 2901 s, 2862 s, 1477 m, 1460 m, 1387 m, 1352 s, 1284 w, 1250 w, 1111 br s, 1078 br s, 1020 s, 962 m, 937 w, 837 w, 754 w, 638 s, 455 w. UV−vis (THF, nm) 224 (ϵ = 3400), 258 (ϵ = 3600), 296 sh (ϵ = 3500), 340 (ϵ = 2800), 530 v br (ϵ = 280). Anal. Calcd for $C_{47}H_{101}KMo_2O_{13}$: C, 51.07; H, 9.21. Found: C, 50.60; H, 9.05.

Synthesis of Monoanion Complex 2a. Solid $W_2(O^tBu)_6$ (1.00 g, 1.24 mmol), KO^tBu (0.14 g, 1.24 mmol), and 18-crown-6 (0.36 g, 1.36 mmol) were weighed into a 30-mL Schlenk flask in the drybox. The flask was immersed in an ice/water bath and THF (~15 mL) was then added to the solid mixture outside the box with the aid of a cannula. The reddish/purple solution was stirred at 0 °C for an additional hour whereupon the volatile components were evaporated *in vacuo* (0 °C, 0.01 Torr). The solid residue was then triturated with several portions (~5 mL) of C_6H_6 and dried *in vacuo* (0 °C, 0.01 Torr). Yield = 1.20 g, 85%. Spectroscopic analysis indicates that the material is pure (>95%) but due to the thermal lability of this complex an elemental analysis was not attempted. For $[K(18\text{-crown-}6)]^+[W_2(O^tBu)_7]^-$ (**2a**): ^1H NMR (C_5D_5N, 300 MHz, 23 °C) δ 3.44 (s, 24H), 1.98 (s, 63H). $^{13}C\{^1H\}$ NMR (C_5D_5N, 75 MHz, 23 °C) δ 77.54 ($-OC(CH_3)_3$), 70.41 ($-OCH_2CH_2-$), 35.22 ($-OC(CH_3)_3$). IR (KBr pellet, cm^{-1}) 2959 s, 2915 s, 1472 w, 1458 w, 1352 s, 1228 m, 1182 s, 1109 s, 964 s, 958 s, 841 w, 798 m. UV−vis (THF, nm) 214 (ϵ = 24000), 264 (ϵ = 6000), 390 sh (ϵ = 1200), 530 v br (ϵ = 400). Deuterated analogus **2a**-d_{63} and **2a**-d_{42} were prepared similarly from $W_2(O^tBu\text{-}d_9)_6$ and $KO^tBu\text{-}d_9$ and $W_2(OC(CH_3)(CD_3)_2)_6$ and $KOC(CH_3)(CD_3)_2$, respectively.

Synthesis of Monoanionic Complex 2b. (a) Synthesis of $W_2(O^iPr)_6$. Solid $W_2(O^tBu)_6$ (0.600 g, 0.744 mmol) was dissolved in hexanes (~15 mL) in a 30-mL Schlenk flask containing a Teflon-coated magnetic stirring bar. The solution was cooled to −50 °C and excess 2-propanol (~1−2 mL) was added with stirring. The solution rapidly turned yellow/golden brown and was stirred for 1 h at this temperature to ensure complete reaction. At this point some yellow solid was evident and the solution was cooled to −90 °C and allowed to stand for 1 h. The yellow microcrystals of $W_2(O^iPr)_6$ were collected by carefully decanting the solvent, washed at low temperature with cold (−90 °C) hexanes (2 × 5 mL), and dried *in vacuo* (23 °C, 0.01 Torr). Yield: 0.440 g, 82%.

(b) Preparation of $[K(18\text{-crown-}6)]^+[W_2(O^iPr)_7]^-$ (2b). Freshly prepared $W_2(O^iPr)_6$ (0.440 g, 0.609 mmol) was weighed into a 30-mL Schlenk flask containing a Teflon-coated magnetic stirring bar along with KO^iPr (0.060 g, 0.610 mmol) and 18-crown-6 (0.205 g, 0.776 mmol). The flask was immersed in a −50 °C cold bath and THF (~15 mL) was added. The resulting yellow solution/white suspension was stirred for 3 h maintaining a temperature of <−30 °C. The reaction darkened over this time and no precipitate was evident at the conclusion of the reaction. The solvent volume was then reduced *in vacuo* to ~7.5 mL and hexanes (~2 mL) were added at room temperature. Upon cooling to −34 °C fan-shaped needles were produced which were collected by carefully decanting the solvent with a cannula, washing with 2 × 5 mL of hexanes, and drying *in vacuo* (23 °C, 0.01 Torr). Yield: 0.560 g, 85%. Due to the thermal lability of this complex elemental analysis was not attempted. For **2b**: ^1H NMR (C_5D_5N, 300 MHz, 23 °C) δ 5.34 (br s, 7H), 3.53 (s, 24H), 1.52 (br s, 42H). $^{13}C\{^1H\}$ NMR (C_5D_5N, 125 MHz, 23 °C) δ 71.72 ($-OCHMe_2$), 70.67 ($-OCH_2CH_2-$), 28.15 ($-OCH(CH_3)_2$). IR (KBr pellet, cm^{-1}) 2957 s, 2907 s, 1458 w, 1354 s, 1319 w, 1251 w, 1113 br s, 970 br s, 837 br m, 596 w, 455 w. UV−vis (THF, nm) 226 (ϵ = 12000), 248 (ϵ = 12000), 384 sh (ϵ = 1600), 466 (ϵ = 730), 540 v br sh (ϵ = 410).

Synthesis of Dianionic Complexes 3c,f. In this case the appropriate $M_2(OCH_2{}^tBu)_6$ complex (or its bis-pyridine adduct: $M_2(OCH_2{}^tBu)_6(py)_2$) and $KOCH_2{}^tBu$ were mixed in a 1:2 ratio and dissolved in THF or pyridine, and the solution was stirred for 1 h. Crystalline material was then obtained by cooling to −34 °C for several days. The crystals were isolated by filtering with a crimped Teflon cannula and washed with additional cold pyridine or THF. The yield of the tungsten complex **3c** is quite high and exceeds 90% if the filtrates are condensed and further crops isolated. The spectroscopic yield for the molybdenum complex is >95%, but the isolated crystalline yield has thus far never exceeded 30% for the first crop. For $K_2W_2(OCH_2{}^tBu)_8$ (**3c**): ^1H NMR (C_5D_5N, 300 MHz, 23 °C) δ 4.19 (s, 16H), 1.18 (s, 72H). $^{13}C\{^1H\}$ NMR (C_5D_5N, 75 MHz, 23 °C) δ 77.26 ($-OCH_2{}^tBu$), 34.24 ($-OCH_2C(CH_3)_3$), 27.82 ($-OCH_2C(CH_3)_3$). IR (KBr pellet, cm^{-1}) 2949 s, 2915 m, 2862 s, 1483 m, 1458 w, 1387 m, 1359 m, 1217 w, 1076 s, 1045 s, 1010 s, 929 w, 898 w, 754 w, 628 s, 445 m. UV−vis (THF, nm) 228 (ϵ = 3300), 256 (ϵ = 3500), 434 br (ϵ = 110), 590 br (ϵ = 130), 816 br (ϵ = 120). Anal. Calcd for $C_{40}H_{88}K_2W_2O_8$: C, 42.03; H, 7.76. Found: C, 42.42; H, 8.16. For $K_2Mo_2(OCH_2{}^tBu)_8$ (**3f**): ^1H NMR (C_5D_5N, 300 MHz, 23 °C) δ 4.19 (s, 16H), 1.19 (s, 72H). $^{13}C\{^1H\}$ NMR (C_5D_5N, 75 MHz, 23 °C) δ 78.46 ($-OCH_2{}^tBu$), 34.34 ($-OCH_2C(CH_3)_3$), 27.84 ($-OCH_2C(CH_3)_3$). IR (KBr pellet, cm^{-1}) 2949 s, 2915 m, 2862 s, 1483 m, 1460 m, 1387 m, 1359 m, 1217 w, 1076 s, 1045 s, 1012 s, 929 w, 897 w, 754 w, 626 s, 449 m. UV−vis (THF, nm) 224 (ϵ = 12500), 242 (ϵ = 12000), 286 (ϵ = 10700), 498 br (ϵ = 200), 682 br (ϵ = 160). Anal. Calcd for $C_{40}H_{88}K_2Mo_2O_8$: C, 49.67; H, 9.17. Found: C, 48.76; H, 8.77.

Oxidation Reactions: (a) Preparation of $Mo_2(O^iPr)_8$. Solid $Mo_2(O^iPr)_6$ (100 mg, 0.183 mmol) and KO^iPr (36 mg, 0.366 mmol) were weighed into a Schlenk flask in the drybox. The flask was sealed and brought out of the box whereupon THF (~12 mL) was added with the aid of a Teflon cannula. The solution immediately turned deep purple as a result of the formation of $[Mo_2(O^iPr)_7]^-$ and the reaction was stirred an additional 1 h. The solvent was evaporated *in vacuo* (23 °C, 0.01 Torr) and the flask brought back in the glovebox. Ph_3PBr_2 (79 mg, 0.183 mmol) was added, followed by ~12 mL of THF, and the reaction mixture was stirred for 8 h. During this time the color changed to a deep green. A white microcrystalline precipitate was filtered (43 mg, 100% of theory for KBr), the solvent was evaporated *in vacuo* (23 °C, 0.01 Torr), and the gooey residue was analyzed by ^1H NMR spectroscopy (C_6D_6, 23 °C) which showed it to consist of at least three molybdenum-containing species: $Mo_2(O^iPr)_8$ (30%, δ 1.38, 5.30 [br s, 48:6H]), $KMo_2(O^iPr)_7Br_2$ (~5%, *vide infra*), and an unknown compound(s) which produced a large/broad signal at δ 2.8 ppm, $w_{1/2}$ = 175 Hz. To date the latter species has eluded definitive characterization. The aryl region of the ^1H NMR spectrum contains only resonances for Ph_3P at δ 7.38 (m, 2H) and 7.02 (m, 3H) consistent with the complete reduction of Ph_3PBr_2. The yield of $Mo_2(O^iPr)_8$ is not improved when clean, recrystallized $[Mo_2(O^iPr)_7]^-$ is used as the starting material along with 1 equiv of KO^iPr and Ph_3PBr_2.

(b) Preparation of $KMo_2(O^iPr)_7Br_2$. Solid $Mo_2(O^iPr)_6$ (150 mg, 0.274 mmol) and KO^iPr (27 mg, 0.274 mmol) were weighed into a 30-mL Schlenk flask containing a Teflon-coated magnetic stirring bar. THF (~12 mL) was added and the reaction mixture was stirred for 1 h. The solvent was evaporated *in vacuo* (23 °C, 0.01 Torr) and Ph_3PBr_2 (118 mg, 0.0274 mmol) was added to the purple crystalline residue. Once again THF was added (~12 mL) and the reaction mixture was stirred for 48 h. The color turned to a deep bluish green. A white microcrystalline precipitate was filtered and the solvent evaporated from the filtrate *in vacuo* (23 °C, 0.01 Torr) to afford a gooey solid which was then dried *in vacuo* (0.01 Torr) at 60 °C for 0.5 h. Toluene (~2 mL) and hexanes (~8 mL) were added to the residue resulting in the formation of a bright blue precipitate which was isolated by filtration, washed with additional hexanes, and analyzed as pure $KMo_2(O^iPr)_7Br_2$ (yield = 56 mg, 30%). For $KMo_2(O^iPr)_7Br_2$: ^1H NMR (toluene-d_8, 300 MHz, 23 °C) δ 11.9 (br m, 1H), 11.0 (br m, 2H), 6.5 (br m, 2H), 3.9 (br m, 1H), 3.7 (br m, 1H), 1.83 (br s, 6H), 1.66 (br s, 6H), 1.42 (br s, 6H), 1.32 (br s, 6H), 1.24 (br s, 6H), 1.15 (br s, 6H), 1.12 (br s, 6H). $^{13}C\{^1H\}$ NMR (toluene-d_8, 75 MHz, 23 °C) δ 25.60, 24.51, 24.07, 23.82, 23.26, 22.40, 21.70 (s, 1:1:1:1:1:1:1 for $-OCH(CH_3)_2$, due to the low solubility of this compound the CH region was not resolved).

IR (KBr pellet, cm^{-1}) 2951 s, 2903 m, 2849 s, 1479 m, 1464 w, 1390 m, 1361 m, 1213 w, 1047 s, 1015 s, 1005 s, 968 m, 931 w, 758 w, 677 s, 665 s, 630 m, 488 w. UV−vis (THF, nm) 208 (ϵ = 4500), 266 (ϵ = 4500), 630 br (ϵ = 330). Anal. Calcd for $C_{21}H_{49}Br_2KMo_2O_7$: C, 31.36; H, 6.14. Found: C, 31.49; H, 6.23.

(c) Preparation of $W_2(OCH_2{}^tBu)_8$. Solid $K_2W_2(OCH_2{}^tBu)_8$ (500 mg, 0.437 mmol) and Ph_3PBr_2 (188 mg, 0.437 mmol) were weighed into a Schlenk flask containing a Teflon-coated magnetic stirring bar. THF was added and the reaction mixture was stirred at 60 °C for 1 h. The reaction mixture turns purple rather quickly and upon cooling both white and purple precipitates are visible. The solids were filtered and washed with THF (1 × 5 mL) and toluene (1 × 5 mL) and dried *in vacuo* (23 °C, 0.01 Torr). The yield at this point is 447 mg, which is presumably contaminated by as much as 103 mg of KBr. IR (KBr pellet) 2953 m, 2904 m, 2866 m, 1479 m, 1390 m, 1361 m, 1215 w, 1045 s, 1014 s, 976 s, 931 m, 756 w, 673 s, 630 m, 480 m, 461 m, 410 w. The mixture was suspended in ~5 mL of toluene and 3 drops of C_5H_5N were added resulting in the formation of a very intensely colored greenish-blue solution and a white precipitate. The latter was filtered (100 mg, 97% based on KBr). Spectroscopically pure material may be isolated by simply evaporating the solvent *in vacuo* (23 °C, 0.01 Torr). At higher temperatures or longer times under dynamic vacuum, reversion to $W_2(OCH_2{}^tBu)_8$ occurs. Yield = 400 mg, 80%. Analytically pure material may be obtained by recrystallization from pyridine at −34 °C for several days. Yield = 210 mg, 42%. For $W_2(OCH_2{}^tBu)_8(py)$: ^1H NMR (C_7D_8, 300 MHz, 80 °C) δ 8.51 (m, 2H), 7.30 (m, 1H), 6.60 (m, 2H), 4.43 (s, 16H), 1.13 (s, 72H). ^1H NMR (C_7D_8, 300 MHz, 23 °C) δ 9.0 (br m, 2H), 7.0 (br m, 1H), 6.7 (br m, 2H), 4.5 (br, 16H), 1.15 (br s, 72H). ^1H NMR (C_7H_8, 300 MHz, −65 °C) δ 9.25 (br m, 2H), 7.05 (br m, 1H), 6.40 (br m, 2H), 5.74 (d, 1H, J = 11 Hz), 5.65 (d, 1H, J = 11 Hz), 5.56 (d, 1H, J = 11 Hz), 5.12 (d, 1H, J = 11 Hz), 4.85 (d, 1H, J = 11 Hz), 4.78 (d, 1H, J = 11 Hz), 4.60 (three overlapping doublets, 3H), 4.05 (d, 1H, J = 11 Hz), 4.01 (d, 1H, J = 11 Hz), 3.88 (d, 1H, J = 11 Hz), 3.59 (d, 1H, J = 11 Hz), 3.53 (d, 1H, J = 11 Hz), 3.38 (d, 1H, J = 11 Hz), 3.02 (d, 1H, J = 11 Hz), 1.46, 1.45, 1.23, 1.20, 0.94, 0.70 (s, 9:9:27:9:9:9 for CH_3). UV−vis (THF, nm) 224 (ϵ = 4700), 244 (ϵ = 4300), 262 (ϵ = 4800), 352 br (ϵ = 2500), 456 br (ϵ = 1600), 656 br (ϵ = 1800). Anal. Calcd for $C_{45}H_{93}NO_8W_2$: C, 47.25; H, 8.19; N, 1.22. Found: C, 46.90; H, 8.10; N, 1.01.

(d) Preparation of $Mo_2(OCH_2{}^tBu)_8$. Solid $K_2Mo_2(OCH_2{}^tBu)_8$ (51 mg, 0.53 mmol) and Ph_3PBr_2 (23 mg, 0.053 mmol) were weighed into a Schlenk flask containing a Teflon-coated magnetic stirring bar. THF (~5 mL) was added and the reaction mixture was stirred overnight. A color change occurs from lavender to deep blue and a white precipitate forms during the course of the reaction. Toluene (~5 mL) was added and the reaction mixture was filtered (10 mg of white solid, theory for KBr is 12 mg). The filtrate volume was reduced to ~2−3 mL and the solution was cooled to −34 °C overnight. The blue microcrystals were isolated by filtration and washed with toluene. Yield = 35 mg, 75%. Contrary to a previous report,[18] pure $Mo_2(OCH_2{}^tBu)_8$ is very insoluble in toluene, and is diamagnetic. ^1H NMR (THF-d_8, 300 MHz, 23 °C) δ 4.3 (br s, 16H), 0.92 (s, 72H). $^{13}C\{^1H\}$ NMR (THF-d_8, 125 MHz, 23 °C) δ 67 (br s, $-OCH_2{}^tBu$), 34.44 s, $-OCH_2C(CH_3)_3$), 28.09 (s, $-OCH_2C(CH_3)_3$). IR (KBr pellet) 2951 m, 2904 m, 2864 m, 1479 m, 1390 m, 1361 m, 1213 w, 1047 s, 1014 s, 1005 s, 968 m, 931 m, 758 w, 681 s, 665 s, 630 m, 488 m, 468 m, 410 w. Anal. Calcd for $C_{40}H_{88}Mo_2O_8$: C, 54.04; H, 9.98. Found: C, 53.88; H, 9.79. Similar to the tungsten analogue, the addition of 1 equiv of pyridine produces a toluene-soluble species. For $Mo_2(OCH_2{}^tBu)_8(py)$: ^1H NMR (C_7D_8, 300 MHz, −7.5 °C) δ 8.51 (m, 2H), 7.00 (m, 1H), 6.70 (m, 2H), 5.77 (s, 2H), 5.24 (br d, 2H), 4.75 (s, 2H), 4.55 (d, 2H, J = 11 Hz), 4.24 (d, 2H, J = 11 Hz), 3.99 (d, 2H, J = 11 Hz), 3.74 (d, 2H, J = 11 Hz), 3.60 (br d, 2H), 1.38 (s, 9H), 1.31 (s, 9H), 1.20 (s, 18H), 1.06 (s, 18H), 0.86 (s, 18H). ^1H NMR (C_7H_8, 300 MHz, −78 °C) δ 9.52, 8.90, 6.52, 6.40, 6.19 (br s, 1H, each for aryl C−H) 5.7 (br d, 1H), 5.47 (br s, 2H), 4.9 (br s, 3H), 4.69 (br s, 2H), 4.35 (br s, 1H), 4.12 (br s, 2H), 3.88 (br s, 2H), 3.80 (br d, 1H), 3.70 (br s, 1H), 2.88 (br s, 1H), 1.98, 1.90, 1.58, 1.42, 0.95, 0.69 (br s, 9:9:27:9:9:9 for CH_3). UV−vis (THF, nm) 232 (ϵ = 4500), 256 (ϵ = 5000), 292 (ϵ = 4800), 434 br (ϵ = 360), 650 br (ϵ = 400).

(e) Preparation of $[K(18\text{-crown-}6)_{1.5}][W_2(\mu\text{-}H)(\mu\text{-}O)(O^tBu)_6]$. Solid $W_2(O^tBu)_6$ (500 mg, 0.620 mmol) and KO^tBu (68 mg, 0.61 mmol) were weighed into a Schlenk flask containing a Teflon-coated magnetic stirring bar in the drybox along with 2 equiv of 18-crown-6 (320 mg, 1.21 mmol). The flask was brought out of the box and THF (~10 mL) was added via cannula resulting in the formation of a purplish solution. The reaction mixture was stirred and heated to 65 °C with the aid of a warm water bath for 2 h resulting in a color change to deep red. The reaction mixture was cooled to room temperature and the solvent evaporated *in vacuo* (23 °C, 0.01 Torr). The reddish solid residue was then treated with ~10 mL of toluene and any unreacted $[K(18\text{-crown-}6)][W_2(O^tBu)_7]$ was removed by filtration. The filtrate volume was condensed *in vacuo* to ~5 mL and ~2 mL of diethyl ether was then added. The solution was then cooled to −34 °C and large crystals deposited over several days. Faster recrystallization may be performed by cooling to −78 °C for several hours, but great care must be taken to follow the recipe described: the product tends to "oil out" unless excess crown ether is present and the solvent is toluene/diethyl ether. Yield 600 mg, 75%. For $[K(18\text{-crown-}6)_{1.5}][W_2(\mu\text{-}H)(\mu\text{-}O)(O^tBu)_6]$: ^1H NMR (300 MHz, C_5D_5N, 23 °C) δ 6.517 (s, 1H, J_{W-H} = 125 Hz), 3.475 (s, 36H), 1.852 (s, 54H). $^{13}C\{^1H\}$ NMR (125 MHz, C_5D_5N, 23 °C) δ 77.40 ($-OC(CH_3)_3$), 69.90 ($-OCH_2CH_2O-$), 33.71 ($-OC(CH_3)_3$). Unfortunately $\nu(W_2(\mu\text{-}H))$ could not be assigned; IR (KBr pellet) 2961, 2910, 1473 w, 1454 w, 1368 w, 1352, 1284 w, 1236, 1180, 1111, 1026 w, 964, 929, 866 w, 837 w, 773 m, 574 w, 511 w, 472 w. For $[K(18\text{-crown-}6)_{1.5}][W_2(\mu\text{-}D)(\mu\text{-}O)(O^tBu)_6]$-$d_{55}$: IR (KBr pellet) 2220 m, 2120 w, 1473 w, 1454 w, 1352 m, 1251 m, 1215 m, ~1120 sh, 1111, 1051, 964, 903, 682 w, 522 w, 426 w. Anal. Calcd for $C_{42}H_{91}KO_{16}W_2$ (1.5 crown ether per K): C, 40.06; H, 7.28. Found: C, 39.98; H, 7.48.

(f) Preparation of $[K(18\text{-crown-}6)][W_2(\mu\text{-}H)(\mu\text{-}O)(O^iPr)_6]$. The experimental details are similar to those described above for the preparation of $[K(18\text{-crown-}6)_{1.5}][W_2(\mu\text{-}H)(\mu\text{-}O)(O^tBu)_6]$. Unfortunately a purification scheme has not been developed to date. For $[K(18\text{-crown-}6)][W_2(\mu\text{-}H)(\mu\text{-}O)(O^iPr)_6]$: ^1H NMR (300 MHz, C_5D_5N, 60 °C) δ 7.10 (s, 1H, J_{W-H} = 130 Hz), 5.51 (hept, 6H), 3.49 (s, 24H), 1.58 (d, 36H). $^{13}C\{^1H\}$ NMR (125 MHz, C_5D_5N, 23 °C) δ 76.16 ($-OCH(CH_3)_2$), 70.60 ($-OCH_2CH_2O-$), 28.00 ($-OCH(CH_3)_2$).

Kinetics for Unimolecular Decomposition of 2a to $[K(18\text{-crown-}6)][W_2(\mu\text{-}H)(\mu\text{-}O)(O^tBu)_6]$ (eq 4). Samples of the appropriate complex anion (**2a**, **2a**-d_{42}, **2a**-d_{63}) were stored in a freezer at −34 °C and were brought into a Helium-filled glovebox just prior to use. Solid **2a** was weighed into an NMR tube to ±0.1 mg accuracy on a Sartorius analytical balance and diluted to 0.60 mL with C_5D_5N. The course of the reaction was monitored by ^1H NMR spectroscopy after allowing the sample to reach thermal equilibrium (see Figure 7) with and without added KO^tBu and found to obey first-order kinetics independent of $[KO^tBu]$ (10^{-1} to 10^{-3} M) which was always present in small amounts due to the reversibility of equilibrium 1. The observed rate constant, k_{obs}, was obtained from plots of $\ln([\mathbf{2a}]/[\mathbf{2a}]_0)$ versus time (see Table 5) at a variety of temperatures (23−80 °C), and the activation parameters determined from an Eyring plot. The thermocouple readings were calibrated with a sample of ethylene glycol and the program TEMCAL(E).[38] Our previously reported values of $\Delta H^\dagger$ = 23.7(5) kcal/mol and $\Delta S^\dagger$ = −3.6(5) eu were found to be slightly altered by the application of a more recent calibration curve. The current values of $\Delta H^\dagger$ = 23.1(5) kcal/mol and $\Delta S^\dagger$ = −3.3(5) eu are thus deemed more reliable, especially with regards to comparison with those values obtained for the decomposition of the isopropoxide complex **2b**. The decomposition of **2a**-d_{63} was followed by ^2H NMR spectroscopy in a similar manner. For **2a**-d_{42}, the decomposition was carried out at the appropriate temperature in the NMR spectrometer until complete. The volatiles were then vacuum distilled into another NMR tube which was then flame-sealed, and a ^1H NMR spectrum was recorded in order to determine the relative ratio of $(CD_3)_2C{=}CH_2$ to $(CH_3)(CD_3)C{=}CD_2$.

Kinetics for Unimolecular Decomposition of 2b to $[K(18\text{-crown-}6)][W_2(\mu\text{-}H)(\mu\text{-}O)(O^iPr)_6]$ (eq 5). The kinetics of this decomposition were measured as described above, but in the temperature range 40−90 °C. The observed rates are tabulated in Table 5 for comparative purposes. When excess KO^iPr was added prior to thermolysis significant rate acceleration was not observed.

Crossover Experiment (Eq 6). The crossover experiment shown in eq 6 was performed similarly, differing only in the fact that 100 equiv of ^tBuOD were added by microliter syringe to a C_5H_5N solution of **2a**. At the conclusion of this reaction the volatiles were vacuum

Table 6. Summary of Crystallographic Data

compd	**2f**·2.5C_6H_6	**3f**·py_2	**3c**·py_2	$[K(18\text{-crown-6})_{1.5}]^+$ $[W_2(\mu\text{-H})(\mu\text{-O})(O^tBu)_6]^-$·tol
empirical formula	$C_{62}H_{131}KMo_2O_{13}$	$C_{50}H_{98}K_2Mo_2N_2O_8$	$C_{50}H_{98}K_2W_2N_2O_8$	$C_{42}H_{91}KO_{16}W_2$; $C_6H_5CH_3$
formula weight	1315.7	1125.41	1269.23	1351.11
color and habit	purple rods	purple plates	blue plates	red bricks
crystal size (mm)	0.25 × 0.25 × 0.35	0.08 × 0.16 × 0.32	0.10 × 0.20 × 0.25	0.20 × 0.25 × 0.40
space group	$P\bar{1}$	$P2_1/c$	$P2_1/c$	$P2_1/n$
unit cell dimens				
a (Å)	19.653(4)	15.683(4)	15.660(3)	15.982(2)
b (Å)	22.244(4)	13.609(3)	13.649(3)	16.617(3)
c (Å)	19.228(3)	29.500(7)	29.502(6)	24.029(4)
α (deg)	110.99(1)	98.23(1)	97.85(1)	97.51(1)
β (deg)	107.51(1)			
γ (deg)	98.19(1)			
temp (°C)	−165	−164	−173	−165
vol (Å^3)	7182.77	6231.12	6246.70	6326.88
Z	4	4	4	4
density (calc g/cm^3)	1.217	1.200	1.270	1.418
abs coef (mm^{-1})	4.492	5.684	36.991	38.309
2θ range (deg)	6−45	6−45	6−45	6−45
reflcns collected	19878	11388	17376	11226
independent reflcns	18439	8165	8186	8272
obsd reflcns	12471 ($F > 2.33\sigma F$)	3310 ($F > 3.0\sigma F$)	6775 ($F > 3.0\sigma F$)	5863 ($F > 3.0\sigma F$)
$R(F)$	0.0666	0.0568	0.0476	0.0763
$R_w(F)$	0.0717	0.0555	0.0405	0.0622
goodness-of-fit	1.667	0.934	1.016	1.258
largest Δ/σ	0.13	0.02	0.01	0.04

distilled and the red residue was analyzed by ^{1}H NMR spectroscopy in C_5D_5N solution. Based on the relative integrals of the (μ-H) and (^{t}Bu) resonances (~54:1 ratio) it was concluded that little, if any, scrambling of the (μ-H) for DO^{t}Bu had occurred during the course of the reaction.

Attempted (μ-H) for (μ-D) Exchange. Solid $[K(18\text{-crown-6})_{1.5}][W_2(\mu\text{-H})(\mu\text{-O})(O^tBu)_6]$ (50 mg, 0.037 mmol) was weighed into a Schlenk flask containing a Teflon-coated magnetic stirring bar. The sample was then dissolved in ~1 mL and 1500 equiv of DO^{t}Bu were added with the aid of a microliter syringe (~4 mL). After stirring at room temperature for 1 h the volatiles were vacuum distilled and the residue analyzed by ^{1}H NMR spectroscopy in C_5D_5N solution. No exchange was detected under these conditions. The reaction was repeated in the presence of 0.5 mg of KO^{t}Bu (0.004 mmol) but the results were the same: no (μ-H) for DO^{t}Bu exchange could be detected.

Reactions of Complex Anions with CO. Solid samples of the appropriate complex anions were weighed into NMR tubes equipped with J. Young valves and dissolved in C_5D_5N or THF-d_8. The samples were freeze−pumped and gaseous carbon monoxide was administered with the aid of a calibrated vacuum manifold (1 equiv). An instantaneous reaction occurs upon thawing the reactions with monoanionic complexes **2d**−**f** as noted by a rapid color change. $^{13}C\{^1H\}$ NMR spectroscopy revealed single resonances for the initial products in the range δ 220−260 ppm, and infrared spectra of the residues showed single bands in the range 1550−1650 cm^{-1}. Complexes **3c** and **3f** failed to react even under forcing conditions (excess ^{13}CO, 65 °C, 12 h, THF-d_8) by NMR spectroscopy. These results are of a preliminary nature and complete characterization data on purified samples will be reported in a future publication.

X-ray Crystallography. Data were collected using previously described procedures.[40] The specific details of each investigation are summarized in Table 6, and a more complete account appears in the supporting information. Pertinent bond distances and angles are provided in Tables 1−4, and a complete listing of these metrical parameters is provided in the supporting information along with listings of fractional coordinates and thermal parameters.

Supporting Information Available: Complete crystallographic details not reported in this paper, tables of fractional coordinates and anisotropic thermal parameters, complete listings of bond distances and angles, and VERSORT/ORTEP drawings showing the complete atom numbering schemes for **2f**, **3f**·py_2, **3c**·py_2, **3c**, and $[K(18\text{-crown-6})_{1.5}][W_2(\mu\text{-H})(\mu\text{-O})(O^tBu)_6]$ (116 pages); complete listings of the observed and calculated structure factors (91 pages). This material is contained in many libraries on microfiche, immediately follows this article in the microfilm version of the journal, can be ordered from the ACS, and can be downloaded from the Internet; see any current masthead page for ordering information and Internet access instructions.

Acknowledgment. We thank Professor Peter T. Wolczanski for providing samples of $NaOSi(^tBu)_3$ and $LiOC(^tBu)_3$ and for helpful discussions. We also thank Professor Charles P. Casey for helpful suggestions. Financial support for the work from the National Science Foundation is gratefully acknowledged.

JA943961K

(40) Chisholm, M. H.; Folting, K.; Huffman, J. C.; Kirkpatrick, C. C. *Inorg. Chem.* **1984**, *23*, 1021.